MED26 regulates the transcription of snRNA genes through the recruitment of little elongation complex

Hidehisa Takahashi[1], Ichigaku Takigawa[2], Masashi Watanabe[1], Delnur Anwar[1], Mio Shibata[1], Chieri Tomomori-Sato[3], Shigeo Sato[3], Amol Ranjan[3], Chris W. Seidel[3], Tadasuke Tsukiyama[1], Wataru Mizushima[1], Masayasu Hayashi[4], Yasuyuki Ohkawa[4], Joan W. Conaway[3,5], Ronald C. Conaway[3,5], Shigetsugu Hatakeyama[1]

[1]Department of Biochemistry, Hokkaido University Graduate School of Medicine, Sapporo, Hokkaido 060-8638, Japan; [2]Creative Research Institution, Hokkaido University, Sapporo, Hokkaido 001-0021, Japan; [3]Stowers Institute for Medical Research, Kansas City, MO 64110, USA; [4]Department of Advanced Medical Initiatives, Kyushu University Graduate School of Medical Sciences, Fukuoka, Fukuoka 812-8582, Japan; [5]Department of Biochemistry and Molecular Biology, University of Kansas Medical Center, Kansas City, KS 66160, USA.

Correspondence: S.H., (hatas@med.hokudai.ac.jp)

Abstract

Regulation of transcription elongation by RNA polymerase II (Pol II) is a key regulatory step in gene transcription. Recently, the little elongation complex (LEC)—which contains the transcription elongation factor ELL/EAF—was found to be required for the transcription of Pol II-dependent *small nuclear RNA* (*snRNA*) genes. Here, we show that the human Mediator subunit MED26 plays a role in the recruitment of LEC to a subset of snRNA genes through direct interaction of EAF and the N-terminal domain (NTD) of MED26. Loss of MED26 in cells decreases the occupancy of LEC at a subset of snRNA genes and results in a reduction in their transcription. Our results suggest that the MED26 NTD functions as a molecular switch in the exchange of TBP-associated factor 7 (TAF7) for LEC in order to facilitate the transition from initiation to elongation during transcription of a subset of snRNA genes.

Introduction

Transcription by RNA polymerase II (Pol II) proceeds through multiple stages, beginning with recruitment of Pol II and other components of the transcription apparatus to the promoter in order to form a preinitiation complex, followed by ATP-dependent unwinding of the DNA template and transcription initiation. Following initiation, Pol II moves away from the promoter, leading to establishment of a productive elongation complex that can complete synthesis of the nascent transcript. Although research for many years was mainly focused on mechanisms that control the preinitiation and initiation stages of transcription[1-3], a growing body of evidence indicates that transcription of many genes is also regulated during transcription elongation[4, 5].

The product of the members of the *eleven-nineteen lysine-rich leukemia* (*ELL*) gene, which is a translocation partner of mixed lineage leukemia (MLL), and its binding partner ELL-associated factors (EAFs) are key regulator of transcription elongation by Pol II[6, 7]. Recently, two distinct ELL/EAF-containing complexes, super elongation complex (SEC) and little elongation complex (LEC), have been identified. SEC contains P-TEFb, ELL/EAF and additional factors, MLL-fusion partner proteins[8-10], and it regulates transcription elongation of a variety of protein-coding genes, including *c-Myc*, *Hsp70*, *Hox* and *HIV* provirus[11]. LEC contains ELL/EAF and additional components, KIAA0947 and NMDA receptor regulated-2 (NARG2), that were also identified as components of Drosophila LEC and are called ICE1 and ICE2 (interacts with C-terminus of ELL), respectively[12]. Recently, it was shown that LEC specifically regulates the transcription of Pol II-transcribed *small nuclear RNA* (*snRNA*) genes[12, 13].

Pol II-transcribed *snRNA* genes are structurally different from Pol II-transcribed protein-coding genes[14]. The promoter is composed of a proximal sequence element (PSE) and an enhancer-like distal sequence element (DSE). In addition, Pol II-transcribed *snRNA* genes

contain a 3'-box instead of a polyadenylation signal, which is required for 3' end formation[15]. Transcription of Pol II-transcribed *snRNA* genes requires an integrator complex that specifically binds to the Ser7-phosphorylated form of the Pol II CTD and proceeds to the 3'end formation[16, 17]. Inhibitors of P-TEFb reduce the 3'-box-dependent 3'end processing but do not affect transcription elongation of the *snRNA* genes[18], indicating that there is different regulation of transcription elongation between Pol II-dependent protein-coding genes and *snRNA* genes.

Mediator is an evolutionarily conserved transcriptional coregulatory complex that is needed for the relay of regulatory signals between gene-specific transcription activators and the basal initiation machinery[19]. Recently, it has been shown that Mediator is involved in the activation of transcription of a number of Pol II-dependent genes at multiple steps, including pre-initiation, promoter clearance, transcription elongation, transcription termination and mRNA splicing steps[20-24]. In metazoan, Mediator is composed of ~30 distinct subunits and exists in multiple and functionally distinct forms that share common core subunits, which are distinguished by the presence or absence of a kinase module composed of Cyclin C, CDK8, MED12 and MED13[25]. Notably, a subset of Mediator contains an additional subunit, MED26. MED26-containing Mediator is copurified with only a small amount of a kinase module but with sub-stoichiometric Pol II, and it plays an important role in gene activation[25-27]. The N-terminal domain (NTD) of MED26 is the most highly conserved region of MED26 and is similar to the NTDs of the elongation factors TFIIS and Elongin A[28, 29]. Previously, we found that MED26 NTD copurifies with two ELL/EAF-containing complexes, SEC and LEC[20]. We showed that MED26 NTD contributes to recruitment of SEC to a subset of human protein-coding genes including *c-Myc* and *Hsp70* through direct interaction of MED26 NTD with EAF[20]. However, generality of the role of MED26 in recruiting ELL/EAF-containing complexes has not been established.

Here, we present evidence that the human Mediator subunit MED26 plays a role in the

recruitment of LEC to a subset of Pol II-transcribed *snRNA* genes through direct interaction of EAF and MED26 NTD. Depletion of MED26 in cells decreases the occupancy of LEC at a subset of *snRNA* genes and results in reduction of expression of the genes. In addition, we identified the MED26 NTD binding region of EAF1. Intriguingly, we found that there is a partially similar amino acid sequence in EAF and TBP-associated factor 7 (TAF7) and that each of the regions is necessary for direct interaction with MED26 NTD. TAF7 has been shown to repress the initiation or post-initiation process of transcription by preventing premature transcription initiation or elongation in a TFIID-dependent or independent manner[30, 31]. Our results indicate that TAF7 directly interacts with MED26 NTD and blocks LEC recruitment to a subset of *snRNA* genes. Based on our findings, we propose a model in which MED26 NTD functions as a molecular switch that interacts with TAF7 in the initiation process and then exchanges it for LEC to facilitate the transition from initiation to elongation during transcription of a subset of *snRNA* genes.

Results

NTD of MED26 is required for interaction with LEC

Since previous mass spectrometric analysis indicated that MED26 NTD interacts with LEC[20], we performed Western blotting to determine whether MED26 NTD is critical for LEC interaction with Mediator. We purified Mediator from HeLa S3 cells stably expressing FLAG-tagged MED26 wild type (WT) or a MED26 NTD deletion mutant (CS: 421-600). Mediator purified through FLAG-MED26-WT or MED26-CS was copurified with Pol II and Mediator components; however, deletion of MED26 NTD resulted in loss of Mediator interaction with LEC components, ICE1 (KIAA0947), ELL and EAF1 (Fig. 1a). Since we previously showed that substitution of two amino acid residues R61 and K62 of MED26 NTD with A interferes with both direct interaction with EAF and interaction with the components of SEC in cells[20], we tested whether the same substitution interferes with the interaction of MED26 NTD and LEC in cells. FLAG-MED26-WT was copurified with LEC, but MED26-R61A, K62A was not (Fig. 1b). These results show that MED26 NTD is critical for interaction of Mediator with LEC. In turn, we tested whether LEC is copurified with MED26-containing Mediator. We purified LEC from 293FRT cells stably expressing FLAG-tagged ICE2 (NARG2). FLAG-ICE2 was copurified with Mediator subunits MED26 and MED1, in addition to ICE1, ELL and EAF1 (Fig. 1c), but FLAG-BTBD19 was not copurified with any of these proteins (Fig. 1c), indicating that LEC interacts with MED26-containing Mediator. Taken together, the results indicate that MED26 NTD functions as a docking site for LEC to recruit it to Mediator.

Purification and reconstitution of little elongation complex

To address the interactions of individual factors within LEC, we expressed FLAG-ICE2,

HA-ICE1, HA-ELL and Myc-EAF1 in the indicated combinations using a baculovirus expression system. FLAG-ICE2 was copurified with HA-ELL only in the presence of HA-ICE1 (Fig. 2a), indicating that ICE1 is required for formation of the protein complex containing ICE1, ICE2 and ELL. Furthermore, HA-ICE1 was copurified with Myc-EAF1 only in the presence of FLAG-ELL (Fig. 2b), indicating that ELL is required for formation of the protein complex containing ICE1, ELL and EAF1. FLAG-ICE2 was copurified with HA-ELL and Myc-EAF1 in the presence of HA-ICE1 (Fig. 2c), indicating that ICE1 is required for formation of the protein complex containing ICE1, ICE2, ELL and EAF1. These results raised the possibility that the largest subunit of LEC, ICE1, functions as a core subunit and connects ICE2 and ELL/EAF for the formation of LEC. Considering that EAF1 directly interacts with MED26 NTD[20], the EAF family protein is thought to function as an adaptor molecule to connect MED26 NTD and LEC (Fig. 2d).

To clarify the region of ICE1 critical for the direct interaction with ICE2 and ELL respectively, we generated recombinant proteins of two truncate mutants of ICE1. The C-terminal fragment of ICE1 (CL: 1191-2266) bound to ICE2, but the N-terminal fragment of ICE1 (NL: 1-1190) did not (Supplementary Fig. 1a). On the other hand, both NL and CL of ICE1 bound to ELL (Supplementary Fig. 1b). These results indicate that the C-terminal fragment of ICE1 is sufficient for the formation of LEC. Consistent with these results, FLAG-tagged ICE1-CL purified from 293FRT cells stably expressing FLAG-ICE1-CL was copurified with LEC components ELL and EAF1 and with Mediator subunits MED26 and MED1 (Supplementary Fig. 1c). Taken together, these findings suggest that the C-terminal fragment of ICE1 (CL: 1191-2266) functions as a core region for the formation of LEC.

LEC enhances transcription elongation of Pol II *in vitro*

To determine whether LEC activates transcription elongation activity of Pol II, we reconstituted LEC using a baculovirus expression system. Since it was difficult to express a sufficient amount of full-length ICE1 (FL: 1-2266) for transcription assays, we used the C-terminal fragment of ICE1 (CL: 1191-2266). HA-ICE1-CL/FLAG-ICE2/FLAG-ELL/Myc-EAF1 complex was reconstituted by a baculovirus expression system (Fig. 2e), and *in vitro* transcription elongation assays were performed to determine whether the complex stimulates Pol II transcription elongation. We used a linearized plasmid with a single-stranded 3' oligo(dC)-tail on its template strand. Although purified Pol II is unable to bind to double-stranded DNA and initiate transcription without assistance from the general transcription factors, it binds to the single-stranded oligo(dC)-tail and initiates transcription specifically at the junction between the single- and double-stranded regions of the template. In the template, the first nontemplate strand (dT) residue is 136 nt downstream of the oligo(dC)-tail, and the next run of (dT) residues is located ≈240 to ≈250 residues from the oligo(dC)-tail (Fig. 2f, upper panel). When transcription was initiated by the addition of purified Pol II, 50 μM ATP, 50 μM GTP, 2 μM CTP and 10 μCi [α-^{32}P]CTP (Fig. 2f, upper panel), labeled 135-nt transcripts paused immediately before the first template T residue accumulated (Fig. 2f, lower left panel, lane 1). After 30 min, reactions were chased with 100 μM CTP and 2 μM UTP in the absence or presence of HA-ICE1-CL/FLAG-ICE2/FLAG-ELL/Myc-EAF1 complex as indicated (Fig. 2f, lower left panel, lanes 2 and 3). When the complex was added with chase nucleotides, the fraction of Pol II that was able to read through the major pause site synthesized longer transcripts (Fig. 2f, lane 3). Quantification of the major paused transcript (#1) and the longer transcript (#2) supports our idea that reconstituted LEC helps Pol II to read through the major pause site and synthesize the longer transcript (Fig. 2f, lower right panel). These results showed that reconstituted LEC enhances transcription elongation of Pol II *in vitro*.

MED26 is required for the occupancy of LEC at *snRNA* genes

To identify the genes in which LEC is present, we performed chromatin immunoprecipitation-sequence (ChIP-seq) analysis of the LEC component ICE1. By plotting the occupancy of ICE1 at the transcription start sites (TSS), we identified 117 genes. Forty-six of these genes were *snRNA* or *snoRNA* genes (Supplementary Data 1). These data are consistent with the results of previous studies showing that LEC plays a role in transcription of Pol II-transcribed *snRNA* genes[12, 13]. To determine whether MED26 plays a role in recruitment of LEC, we performed ChIP-seq analysis of ICE1 using chromatin from HEK293T cells that had been transfected with control siRNA or MED26 siRNA. By plotting the occupancy of ICE1 at known TSS in cells treated with control siRNA, a subset of *snRNA* and *snoRNA* genes was shown to be occupied by ICE1 (Fig. 3a-d, Supplementary Fig. 2a-c and Supplementary Data 2). Upon siRNA-mediated depletion of MED26, almost all of the ChIP peaks of ICE1 at *snRNA* genes were decreased (Fig. 3a-d and Supplementary Fig. 2a-c), indicating that MED26 is critical for the occupancy of ICE1 at a subset of *snRNA* genes. In control experiments, we confirmed that MED26 depletion had no significant effect on the expression of Mediator subunit MED1, any of LEC components tested and Pol II subunit Rpb1 (Fig. 3e). Next, we performed ChIP-qPCR of ICE1 using probes for a subset of *snRNA* genes and *CELF3* gene in which peaks of ICE1 were detected in ChIP-seq analysis (Supplementary Data 1 and Data 2) and using the Pol III-transcribed *U6* gene as a negative control. Consistent with the results of ChIP-seq analysis of ICE1, ICE1 was significantly occupied at the *U1-1*, *U4-1*, *U5A*, *U5B snRNA* genes and *CELF3* gene compared to the *U6 snRNA* gene (Fig. 3f). MED26 knockdown decreased the occupancy of ICE1 significantly at *U1-1*, *U4-1*, *U5A* and *U5B snRNA* genes but not at the *CELF3* gene (Fig. 3f), indicating that depletion of MED26 specifically decreased the occupancy

of ICE1 at a subset of *snRNA* genes. MED26 knockdown decreased the occupancy of other LEC components, ELL and EAF2, at *U1*, *U4-1*, *U5A* and *U5B snRNA* genes (Fig. 3f). These data show that MED26 is required for the occupancy of LEC at a subset of *snRNA* genes.

Transcription of *snRNA* genes by Pol II is associated with Ser7 phosphorylation of Pol II CTD[16]. Depletion of MED26 decreased the occupancy of total Pol II (Rpb1), accompanied by a decrease in the occupancy of Ser7-phosphorylated Pol II at *snRNA* genes (Fig. 3f). These results suggest that MED26 contributes to Pol II recruitment and/or Ser7 phosphorylation of Pol II CTD at *snRNA* genes.

MED26-containing Mediator is present at *snRNA* genes

To test whether Mediator was present at *snRNA* genes, we performed ChIP of Mediator subunits, MED26, MED23 and MED1, followed by qPCR using probes for the *c-Myc* gene and *snRNA* genes including *U1-1*, *U4-1*, *U4-2*, *U5A*, *U5B* and *U6* (Fig. 4a). Consistent with the results of a previous study showing that MED26 plays a role in recruitment of SEC to the *c-Myc* gene, MED26, MED23 and MED1 were present at the promoter region of the *c-Myc* gene (Fig. 4b). Significantly larger amounts of MED26, MED23 and MED1 were present at *snRNA* genes including *U1-1*, *U4-1*, *U4-2*, *U5A* and *U5B* than those at the upstream or downstream regions of the respective genes and *U6 snRNA* gene (Fig. 4b). These results showed that Mediator was present at a subset of *snRNA* genes.

It was previously shown that LEC was colocalized at Cajal bodies[13]. Cajal bodies were shown to be the sites for not only pre-mRNA splicing but also transcription of *snRNA* genes[32]. We therefore investigated whether MED26 was also colocalized with coilin, which is widely used as a molecular marker of Cajal bodies. We performed immunostaining of ICE1 and MED26 using HeLa cells. ICE1 was colocalized with coilin in Cajal bodies (Supplementary Fig.

3). MED26 was stained diffusely in the nucleus and partly formed nuclear dots in which coilin was colocalized (Fig. 4c). These results indicate that MED26-containing Mediator is colocalized with coilin at Cajal bodies and are consistent with our idea that MED26 has a role in transcription of *snRNA* genes.

MED26 is required for the expression of *snRNA* genes

To test whether depletion of MED26 affects the expression of *snRNA* genes, total RNAs were extracted from HEK293T cells that had been transfected with control siRNA or one of three different MED26 siRNAs (Supplementary Fig. 4a). qRT-PCR analysis revealed that the expression of a subset of *snRNA* and *snoRNA* genes, including *U1*, *U2*, *U4-1*, *U4-2*, *U5A*, *U5B*, *U11* and *snord118*, was decreased following transfection of all three MED26 siRNAs, but the expression of *U6 snRNA* genes was not changed by depletion of MED26 (Fig. 5a). These findings show that MED26 is required for the expression of *snRNA* genes.

To assess the potential contribution of MED26 NTD to the transcription of *snRNA* genes, we generated mouse embryonic fibroblast (MEF) cells from day 10.5 homozygous embryos in which a gene trapping construct had been inserted into the first intron of the mouse *MED26* gene. Consistent with the results of a recent study showing that MED26 is critical for organismal viability but not for cell survival in *Drosophila*[33], MEF cells from MED26 gene trap homozygous embryos were alive and expressed house-keeping protein GAPDH and Mediator subunit MED18 at levels similar to those in MEF cells from wild-type embryos. In contrast, the expression of MED26 in MEF cells was undetectable unlike that in wild-type embryos (Supplementary Fig. 4b). To investigate the contribution of MED26 NTD to *snRNA* gene expression in cells, MED26 wild type and MED26-R61A, K62A, which did not interact with LEC (Fig. 1b), were stably expressed in MEF cells from MED26 gene trap homozygous

embryos. We confirmed that MED26-R61A, K62A was expressed at the same level as that of MED26 wild type and that it had no significant effect on the expression of MED1, Rpb1 and heat shock protein 90 (Hsp90) (Supplementary Fig. 4c). The expression levels of mouse *U1A1*, *U2*, *U3B*, *U5G* and *U11 snRNA* genes, but not the expression level of the *U6 snRNA* gene, were significantly higher in MEF cells expressing MED26 wild type than in MEF cells expressing MED26-R61A, K62A (Fig. 5b). These results indicate that MED26 NTD contributes to the expression of *snRNA* genes through the recruitment of LEC.

Region of EAF1 necessary for interaction with MED26 NTD

Since we previously found that EAF1 directly bound to MED26 NTD[20], we carried out an experiment to determine the region of human EAF1 responsible for interaction with MED26 NTD. We tested whether recombinant proteins of a series of HA-EAF1 C-terminal deletion mutants bound to FLAG-MED26 NTD (Fig. 6a). The full length (FL) of EAF1 bound to MED26 NTD, but the C-terminal deletion mutant N244 did not (Fig. 6b), indicating that carboxyl terminal amino acid residues from 245 to 268 in human EAF1 are required for interaction with MED26 NTD.

Comparison of MED26 NTD binding regions in EAF and TAF7

Since we previously found that EAF and TFIID bind to the overlapping binding site of MED26 NTD and that EAF1 recruitment by Mediator is inhibited by TFIID *in vitro*[20], we considered the possibility that a certain TBP-associated factor (TAF) directly interacts with MED26 NTD. First, we investigated which TAFs directly interact with MED26 NTD. We performed *in vitro* binding assays using bacterially expressed GST-tagged MED26 and a pool of 13 kinds of human TAFs (from TAF1 to TAF13) expressed in a baculovirus expression system and tested which TAFs

were pulled down by GST-MED26. We found that TAF1 and TAF7 were copurified with GST-MED26 but not with GST alone. To test whether TAF7 directly interacts with MED26 NTD, we performed *in vitro* binding assays using bacterially expressed FLAG-MED26 NTD and HA-TAF7. TAF7 directly interacted with MED26 NTD but not with MED26 NTD R61A, K62A (Supplementary Fig. 5a). In turn, TAF1 bound to MED26 NTD only in the presence of TAF7 (Supplementary Fig. 5b), suggesting that TAF1 interacted with MED26 NTD via TAF7 in the first binding assay with pooled TAFs. This result indicates that MED26 NTD interacts with not only free TAF7 but also TAF7 bound to TAF1, raising the possibility that MED26 NTD interacts with TAF7 in the context of TFIID. Since TAF7 is a subunit of TFIID, it is possible that expression of TAF7 as a single subunit results in aggregation and that recombinant protein of TAF7 does not exist as a monomer. To exclude this possibility, we tested whether recombinant HA-TAF7 and FLAG-TAF7 bind to each other. An *in vitro* binding assay revealed that HA-TAF7 bound to FLAG-MED26-NTD but not to FLAG-TAF7 (Supplementary Fig. 5c). Although it is still possible that recombinant TAF7 proteins form a higher order state and do not bind to each other, our results suggest that recombinant TAF7 exists at least in part as a monomer. Taken together, our results showed that TAF7 directly bound to MED26 NTD.

Next, we investigated whether TAF7 harbors an amino acid sequence similar to that of the MED26 NTD binding region of EAF1. Sequence alignment revealed that the amino acid sequence from 219 to 235 in human TAF7 is partially similar to the amino acid sequence from 253 to 268 in human EAF1 (Fig. 6c). Notably, both of the regions in TAF7 and EAF are conserved among species (Fig. 6c). To determine whether the region of TAF7 is responsible for interaction with MED26 NTD, we generated recombinant proteins of a series of HA-TAF7 C-terminal deletion mutants (Fig. 6d) and FLAG-MED26 NTD by a baculovirus expression system and tested whether these mutants bind to MED26 NTD. FL and N243 (1-243) of TAF7

bound to MED26 NTD, but N202 (1-202) and N129 (1-129) did not (Fig. 6e), demonstrating that the region from 203 to 243 is required for interaction with MED26 NTD. We next tested whether the same region of TAF7 is required for interaction with MED26 in cells. FLAG-TAF7 FL and a series of C-terminal deletion mutants were purified from HeLa S3 cells stably expressing each of TAF7 FL and deletion mutants. FLAG-tagged FL and N243 were copurified with MED26, but N202 and N129 were not (Fig. 6f), demonstrating that the region from 203 to 243 is required for interaction with MED26 in cells.

Consistent with results of previous studies showing that the amino acid sequence from 139 to 249 of TAF7 contributes to the binding site for TAF1[34-36], FLAG-TAF7 FL, N243 and N202 were copurified with TFIID components TAF1 and TBP, but N129 was not (Fig. 6f). These findings indicate that the region from 203 to 243 of TAF7 is dispensable for interaction with TAF1 or TFIID. Our results indicate that the distinct region of TAF7 contributes to interaction with MED26 and its incorporation into TFIID.

Point mutations of TAF7 and EAF1 block binding to MED26 NTD

We generated point mutants of EAF1 and TAF7 which lose interaction with MED26 NTD (Fig. 7a). Mutations of S262, G263, S264 and D265 to A interfered with the interaction of EAF1 and MED26 NTD (Fig. 7b). Similarly, mutations of S229, S230, E231 and D232 to A interfered with the interaction of TAF7 and MED26 NTD (Fig. 7c). Consistent with the fact that the region of TAF7 is not well conserved in TAF7L (Fig. 7a), TAF7L did not bind to MED26 NTD (Fig. 7d). To test whether the region of TAF7 is critical for interaction with MED26 in cells, we generated HeLa cells stably expressing FLAG-tagged TAF7 wild type and point mutant (S229A, S230A, E231A, D232A) and purified TFIID (Fig. 7e). Consistent with our results showing that the region of TAF7 is dispensable for interaction with TFIID (Fig. 6f), both the wild-type and

point mutant copurified with similar levels of TFIID components TAF1 and TBP (Fig. 7f). In contrast, the wild type of TAF7 copurified with MED26 and MED1, but the point mutant did not (Fig. 7f), demonstrating that the region of TAF7 is required for interaction with MED26-containing Mediator. These findings indicate the possibility that TAF7 in the context of TFIID and/or free TAF7 interact with MED26-containing Mediator.

TAF7 is present at *snRNA* genes

To test whether TAF7 is also present at *snRNA* genes, we compared the peaks of ICE1 (KIAA0947) ChIP-seq and TAF7 ChIP-seq. We identified 2912 TAF7-bound genes by TSS analysis (Fig. 8a and Supplementary Data 3). Forty-two genes out of the 117 ICE1-bound genes overlapped with TAF7-cooccupied genes. Notably, most of the 42 genes were *snRNA* or *snoRNA* genes (Fig. 8a and Supplementary Data 4), indicating that TAF7 plays a role in regulating the transcription of *snRNA* genes. TAF7 was colocalized with ICE1 at a subset of *snRNA* genes (Fig. 8b-e and Supplementary Fig. 6a-c). ChIP-qPCR analysis also demonstrated that TAF7 was present at a subset of *snRNA* genes (Fig. 8f).

Knockdown of TAF7 increases LEC recruitment to *snRNA* genes

Next, we tested how depletion of TAF7 in cells affects the expression of *snRNA* genes. We performed qRT-PCR to analyze *snRNA* gene expression in HEK293T cells in which TAF7 had been depleted by transient transfection of siRNA (Fig. 9a). Knockdown of TAF7 mildly increased the expression of *snRNA* genes (Fig. 9b).

Since partially similar amino acid sequences of TAF7 and EAF1 contribute to interaction with MED26 NTD, we considered the possibility that EAF1 and TAF7 bind to MED26 NTD in a mutually exclusive manner and that TAF7 inhibits EAF1 recruitment by Mediator. To test this

possibility, we performed an immobilized template recruitment assay using an oligo(dC)-tailed template immobilized on Streptavidin beads (Fig. 9c). Since sub-stoichiometric Pol II is copurified with MED26-containing Mediator and Pol II binds to the single-stranded oligo(dC)-tail, MED26-containing Mediator binds to the oligo(dC)-tailed template via Pol II without any assistance of DNA-binding transcription activators. Using the template, we tested whether MED26-containing Mediator recruits EAF1 to the template (Supplementary Fig. 7a). MED26-containing Mediator recruited EAF1 to the template, but MED26 mut (R61A, K62A)-containing Mediator did not (Supplementary Fig. 7b). Next, we performed immobilized template assays in the presence and absence of MED26-containing Mediator and recombinant proteins of EAF1 and N243 of TAF7 and tested whether TAF7 inhibits EAF1 recruitment by MED26-containing Mediator (Fig. 9c). TAF7 N243 inhibited EAF1 recruitment by Mediator in a dose-dependent manner (Fig. 9d), indicating that TAF7 N243 binds to MED26 NTD and blocks EAF1 recruitment (Fig. 9e).

Next, we tested whether TAF7 knockdown increases the occupancy of LEC at *snRNA* genes in cells. TAF7 depletion moderately increased the occupancy of the components of LEC including ICE1, EAF2 and Pol II at *U4-1* and *U5B snRNA* genes (Fig. 9f), but it did not affect the occupancy of MED1 and MED26 at *snRNA* genes (Supplementary Fig. 7c). These findings suggest that TAF7 plays a role in repression of the transcription of a subset of *snRNA* genes through interfering with the recruitment of LEC to a subset of Pol II-transcribed *snRNA* genes.

Discussion

In this report, we present evidence that the human Mediator subunit MED26 contributes to the recruitment of LEC to a subset of Pol II-transcribed *snRNA* genes. MED26 depletion in cells decreased the expression of *snRNA* genes and the occupancy of LEC components at the genes. Molecular genetic approaches using MEF cells from MED26 gene trap homozygous embryos have revealed that wild-type MED26 contributes more to the expression of *snRNA* genes than does a MED26 point mutant that does not interact with LEC. Our results indicate that Mediator plays a crucial role in the transcription of *snRNA* genes through recruitment of LEC. Our results are also consistent with evidence that a meta-coactivator complex (MECO) containing Mediator and Ada-Two-A-containing histone acetyltransferase (ATAC) play a role in transcription of a subset of *snRNA* genes in mouse ES cells[37]. In a recent study, LEC was copurified with TFIIH[38]. Notably, knockdown of ELL as well as components of TFIIH reduced global RNA synthesis after UV irradiation, indicating that ELL plays a role in the restart of transcription after transcription-coupled DNA repair (TCR)[38]. This evidence indicates the possibility that LEC plays a role in TCR in *snRNA* gene transcription. Our results indicate that Mediator can function as a key coordinator by orchestrating multiple coregulator complexes and regulate the expression of a subset of *snRNA* genes possibly through activating transcription elongation and/or reactivating paused Pol II after TCR.

This study and our previous research suggest that MED26 NTD contributes to the recruitment of SEC and LEC to Pol II-transcribed protein-coding genes and *small nuclear RNA* genes, respectively, through direct interaction with EAF[20]. However, the hypothesis does not completely explain the mechanisms by which target genes of SEC and LEC are determined, because EAF is a shared component of both SEC and LEC. It is conceivable that other factors

also contribute to the determination of target genes of SEC or LEC. A recent study showed that depletion of ICE1 also decreased the occupancy of other LEC components at *snRNA* genes, indicating that ICE1 functions as a scaffold protein for LEC and contributes to the recruitment of LEC to the promoter[13]. It has also been reported that the minor difference in U1 and U6 promoters results in a slight conformational change of SNAPc and could determine the Pol II and Pol III specificities of the U1 and U6 promoters[39]. The results of those studies and our study raise the possibility that a combination of MED26, ICE1, SNAPc and other factors contributes to the LEC recruitment to *snRNA* genes. It has been shown that LEC contains additional components, UPSL1 and ZC3H8[12, 13, 40]. In our mass spectrometric analysis of MED26 NTD-interacting proteins, we identified ICE1 (KIAA0947), ICE2 (NARG2), ELL and EAF, but not UPSL1 and ZC3H8, as interacting proteins[20], suggesting that a form of LEC composed of ICE1, ICE2, ELL and EAF is recruited to the promoters by Mediator.

We found that EAF and TAF7 harbor a partially similar amino acid sequence that is necessary for direct interaction with MED26 NTD. We presented evidence that TAF7 is present at a subset of *snRNA* genes. We found that TAF7 blocks EAF1 recruitment by Mediator *in vitro* and that depletion of TAF7 in cells increased the occupancy of LEC and Pol II at a subset of *snRNA* genes, resulting in an increase in the expression of the genes. Our results are consistent with results of previous studies showing that TAF7 has a role in repression of the transcription of a subset of genes[30, 41]. TAF7 was shown to inhibit TAF1 acetyltransferase activity, which is necessary for transcription initiation. The release of TAF7 from TFIID allows transcription initiation, indicating that TAF7 functions as a checkpoint factor of transcription initiation and represses TFIID-dependent transcription initiation by preventing premature transcription initiation[35]. It has also been shown that depletion of Mediator subunits decreases transcription of the *metallothionein A* gene and that depletion of both TAFs and Mediator subunits restores the

transcription[42], suggesting that transcription of the gene is regulated by the balance of TFIID and Mediator. That report is consistent with our results suggesting that the transcription of a subset of *snRNA* genes is regulated by the balance of TAF7-containing TFIID and MED26-containing Mediator. TBP and some of the TBP-associated factors (TAFs) have been shown to be involved in the transcription of *snRNA* genes[43, 44]. Our results raise the possibility that TAF7 in the context of TFIID is involved in *snRNA* gene transcription; however, further experiments are needed to address the precise composition of the form of TBP-TAFs in *snRNA* gene transcription.

The results of our study raise the possibility that TAF7 occludes the MED26 NTD and interferes with the recruitment of LEC in the step of initiation or the very early step of elongation to prevent premature transcription elongation. After TAF7 is released from MED26 NTD upon an appropriate signal, LEC can be recruited to the genes through direct interaction of EAF and MED26 NTD to facilitate the transition from initiation to elongation in transcription of a subset of *snRNA* genes (Fig. 10).

Methods

Cell culture

Human embryonic kidney 293T cells, HeLa cells, HeLa S3 cells and their derivatives, and Flp-In 293 cells (Invitrogen, Carlsbad, CA) and their derivatives were cultured under an atmosphere of 5% CO_2 at 37°C in DMEM (Sigma-Aldrich Corp., St Louis, MO) supplemented with 10% (v/v) fetal bovine serum (Invitrogen), 55 μM β-mercaptoethanol (GIBCO, Grand Island, NY), 2 mM L-glutamine, penicillin (10 U ml^{-1}) and streptomycin (0.1 mg ml^{-1}). Generation of a HeLa S3 cell line stably expressing FLAG-tagged MED26 wild type, CS (421-600) and R61A, K62A, and Flp-In 293 cells stably expressing FLAG-tagged ICE2, ICE1-CL (1191-2266) were described previously[20].

Production of recombinant proteins

N-terminally 6xHis- and FLAG-tagged MED26-NTD (residues 1-113), MED26-NTD R61A, K62A, and N-terminally 6xHis- and HA-tagged TAF7 were expressed in BL21 (DE3) CodonPlus *Escherichia coli* (Stratagene, La Jolla, CA) and then purified by using ProBond metal affinity beads (Invitrogen). For production of recombinant proteins in Sf9 cells, epitope-tagged ELL, EAF1 and MED26 were subcloned into pBacPAK8 expressed using the BacPAK system (Clontech Laboratories, Inc. Mountain View, CA). Full length, deletion mutants or point mutants of ICE1 (KIAA0947), ICE2 (NARG2), MED26, TAF7 and EAF1 were subcloned into pFastBac HTb (Life Technologies, Carlsbad, CA) or pBacPAK8 with epitope tags and expressed singly or together with the BAC-to-BAC system (Clontech).

Western blotting

Anti-FLAG M2 antibodies (1:2000 dilutions, Sigma-Aldrich Corp.), anti-HA antibodies (1:2000 dilutions, Covance, Princeton, NJ), anti-Myc antibodies (1:1000 dilutions, Covance), anti-TAF7 antibodies (1:200 dilutions, sc-101167, Santa Cruz Biothecnology, Santa Cruz, CA), anti-ELL antibodies (1:1000 dilutions, A301-645A, Bethyl Laboratories, Montgomery, TX), anti-EAF2 antibodies (1:1000 dilutions, A302-502A-1, Bethyl Laboratories), anti-Rpb1 antibodies (1:2000 dilutions, sc-899 X, Santa Cruz) and anti-MED1 antibodies (1:2000 dilutions, sc-5334 X, Santa Cruz) were used in Western blots. Mouse monoclonal anti-EAF1 antibody (1:500 dilutions) was a gift from Michael Thirman (Department of Medicine, University of Chicago).

Immunoprecipitation and affinity purification

Protein complexes were purified from nuclear extracts or S100 fractions of cell lines stably expressing FLAG-tagged proteins using anti-FLAG M2 agarose (Sigma-Aldrich Corp.) as described previously[45]. Briefly, nuclear extracts and S100 fractions were prepared according to the method of Dignam et al.[46] from parental HeLa cells or HEK293 FRT cells stably expressing FLAG-tagged proteins. Each of the nuclear extracts or S100 fractions was incubated with 100 μl anti-FLAG agarose beads for 2 hr at 4°C. The beads were washed 5 times with a 100-fold excess of a buffer containing 50 mM Hepes-NaOH (pH 7.9), 0.3 M NaCl, 0.1% Triton X-100, and 10% (v/v) glycerol and then eluted with 100 μl of a buffer containing 0.1 M NaCl, 50 mM Hepes-NaOH (pH 7.9), 0.05% Triton X-100, 10% (v/v) glycerol and 0.25 mg ml^{-1} FLAG peptide.

Oligo(dC)-tailed template transcription assay

Transcription reactions were carried out in the presence of 20 mM Hepes-NaOH, pH 7.9/20 mM Tris-HCl, pH 7.9/60 mM KCl/2 mM DTT/0.5 mg ml^{-1} BSA/1% (wt/vol) polyvinyl alcohol

(average molecular weight of 30,000–70,000 Da)/3% (wt/vol) glycerol/8 units of RNasin/8 mM $MgCl_2$/25 ng oligo(dC)-tailed pAd-GR220/~0.01 unit Pol II, and ribonucleoside triphosphates and transcription factors as indicated in the figures. In the experiments for which results are shown in Fig. 2f, reaction mixtures were preincubated for 30 min at 28°C before the addition of ribonucleoside triphosphates. Reactions were stopped after incubation at 28°C for the times indicated in the figure, and products were resolved on 6% polyacrylamide gels containing 7 M urea, 45 mM Tris-borate and 1 mM EDTA (pH 8.3).

Generation of mouse embryonic fibroblast cells

ES cell line RRR660, in which the gene trapping construct pGT0lxf had been inserted into the first intron of one allele of the mouse *MED26* gene, was purchased from Mutant Mouse Regional Resource Center (MMRRC) at JAX. The ES cell line was injected into blastocysts of C57BL/6 mice, and chimera mice were generated. After heterozygous mice had been generated, homozygous embryos were generated by mating heterozygous mice. The embryos were covered in PBS, and the placenta, other maternal tissues, head, limbs and all innards were removed and then homogenized with a 22 gauge syringe. Mouse embryonic fibroblast (MEF) cells were then cultured under an atmosphere of 5% CO_2 at 37°C in DMEM (Sigma-Aldrich Corp.) supplemented with 10% (v/v) fetal bovine serum (Invitrogen), 55 μM β-mercaptoethanol (GIBCO, Grand Island, NY), 2 mM L-glutamine, penicillin (10 U ml^{-1}) and streptomycin (0.1 mg ml^{-1}). MED26 gene trap MEF cell lines stably expressing HA-tagged MED26 wild type (wt) or mutant (R61A, K62A) were generated by a Plat E retrovirus packaging system[47].

Immobilized oligo(dC)-tailed template assays

A biotinylated oligo(dC)-tailed template generated from the plasmid pAd-GR220 was

immobilized on Dynabeads™ (Life Technologies). Promoter binding assays were performed as follows. Various combinations of proteins were incubated with 2.0 µl of Dynal beads in a reaction mixture containing 62.5 mM KCl/ 12.5% v/v glycerol/ 12.5 mM HEPES, pH 7.9/ 20 mM Tris-HCl pH 7.9/ 0.06 mM EDTA, pH 8.0/ 7.5 mM $MgCl_2$/ 0.5 mg ml^{-1} BSA/ 0.3 mM DTT/ 0.025 % NP40 in a total volume of 60 µl. After 30 minutes at 28 °C, beads were collected using a magnetic particle concentrator (Life Technologies), washed 3 times in the same buffer without BSA, and resuspended in SDS-PAGE loading buffer. Bound proteins were identified by Western blotting[45].

Gene expression analysis

Total RNA was isolated using Isogen II (Nippon gene, Tokyo, Japan). For RT-qPCR, total mRNA was reverse-transcribed using the iScript Select cDNA Synthesis Kit (Biorad, Hercules, CA). The threshold cycle (Ct) values were determined by real-time PCR reactions using an Applied Biosystems StepOne Realtime PCR System and Power SYBR Green PCR Master Mix (Life Technologies) and normalized by subtracting the Ct value of the GAPDH gene from the Ct value of the respective gene ($\Delta Ct = Ct^{gene} - Ct^{GAPDH}$). The relative mRNA levels were then calculated using $2^{-\Delta Ct}$. Primer sequences are listed in PCR primers of Supplemental information.

ChIP assays.

Cells from one 10-cm dish (~1 x 10^7) of HEK293T cells grown to 70-80% confluence were used for each immunoprecipitation. The cells were cross-linked with 2 mM DSG Crosslinker (c1104, ProteoChem, Loves Park, IL) in PBS for 30 min and then 1% formaldehyde in PBS for 20 min at room temperature. Then the cells were resuspended and lysed in lysis buffer (0.2% or 0.5% SDS, 10 mM EDTA, 150 mM NaCl, 50 mM Tris-HCl pH 8.0), and they were sonicated

with a Bioruptor® Sonicator (Diagenode, Denville, NJ) for 15 or 30 times for 30 seconds at the maximum power setting to generate DNA fragments of ~150-500 bps. Sonicated chromatin was incubated at 4°C overnight with 5-10 µg of normal IgG or specific antibodies. Specific antibodies used were as follows: MED26 (H-228, sc-48776 X, Santa Cruz), MED23 (A300-425A-1, Bethyl Laboratories, Montgomery, TX), ICE1 (raised against bacterially expressed, His-tagged recombinant proteins of ICE1 1865-2266 aa), ELL (A301-645A, Bethyl Laboratories), EAF2 (A302-502A-1, Bethyl Laboratories), TAF7 (SQ-8, sc-101167, Santa cruz), Rpb1 (N20, sc-899, Santa Cruz) and RNA Pol II CTD phospho Ser7 (Cat# 61087, Active motif, Carlsbad, California). Then rProtein A Sepharose^{TM} (17-1279-02, GE Healthcare, Pittsburgh, PA) was added and incubated for 2 hr at 4°C. The beads were washed 2 times with IP buffer (20 mM Tris-HCl pH 8.0, 150 mM NaCl, 2 mM EDTA, 1% Triton X-100), 2 times with high salt buffer (20 mM Tris-HCl pH 8.0, 500 mM NaCl, 2 mM EDTA, 1% Triton X-100), once with LiCl buffer (250 mM LiCl, 20 mM Tris-HCl pH 8.0, 1 mM EDTA, 1% Triton X-100, 0.1% NP40 and 0.5% NaDOC) and 2 times with TE buffer. Bound complexes were eluted from the beads with 100 mM $NaHCO_3$ and 1% SDS by incubating at 50°C for 30 min with occasional vortexing. Crosslinking was reversed by overnight incubation at 65°C. Immunoprecipitated DNA and input DNA were treated with RNase A and Proteinase K by incubation at 45°C. DNA was purified using the QIAquick PCR purification kit (28106, Qiagen, Valencia, CA) or MinElute PCR purification kit (28006, Qiagen). Immunoprecipitated and input material was analyzed by quantitative PCR. ChIP signal was normalized to total input. Three biological replicates were performed for each experiment. Primer sets are detailed in Supplemental Information.

ChIP-seq and gene annotation

Sequencing reads were acquired through primary Solexa image analysis. Filtered leads were then aligned to the human genome (hg19) using the Bowtie alignment tool. Only those sequences that matched uniquely to the genome with up to two mismatches and mapped to less than 3 locations were retained for subsequent analyses. Sequence reads for each ChIP-sequence data set and its associated whole-cell extract controls were used for Input. Sequence reads from triplicate or single ChIP-sequence data set of ICE1 (KIAA0947) or TAF7 were used in analysis with the MACS2 peak finding program version 2.0.10, and significantly enriched regions of ChIP-sequence signals were determined. Three of each data set from triplicate samples was summed up using MACS2. The significance cutoff was set to FDR<1% and a fold change between 5 and 50. All other MACS parameters were left default. Genes were identified if an enriched peak region was found within ±1kbp of the TSS of any transcript isoform of the gene. The txStart positions of the Ensembl gene annotation were used for TSS analysis.

siRNA transfection

HEK293T cells in 6-well tissue culture plates (~$1x10^5$ cells/well) or 10 cm dishes (~2 $x10^6$ cells/dish) were transfected with 50 nM siRNAs targeting human MED26 (#1, s18074; #2, s18075; #3, s18076, Ambion/Life Technologies), with 50 nM of siRNA targeting human TAF7 (ON-TARGET plus SMART pool, L-013669-00, Dharmacon, Pittsburgh, PA) or with 50 nM siGENOME NON-TARGETING siRNA Pool #2 (D-001206-14, Dharmacon) using Lipofectamine™ RNAiMAX Transfection Reagent (Invitrogen).

Immunostaining

HeLa cells grown on glass coverslips were fixed for 7 min at room temperature with 100% methanol. Then the cells were incubated for 15 min with PBS containing 0.2% Triton X-100.

After blocking cells with TBST containing 3% BSA, the cells were incubated at room temperature with primary antibodies to coilin (ab11822, Abcam, Cambridge, UK) at 1:1000 dilutions, MED26 (H228, sc-48776 X, Santa Cruz) at 1:2000 dilutions, or ICE1 (KIAA0947) at 1:1000 dilutions in TBST containing 3% BSA. The cells were then incubated with Alexa488-labeled goat polyclonal antibody to mouse IgG or Alexa546-labeled goat polyclonal antibody to rabbit IgG (Life Technologies), covered with a drop of VECTASHIELD (VECTOR Laboratories, Burlingame, CA), and then photographed with a CCD camera (DP71, Olympus, Japan) attached to an Olympus BX51 microscope.

References

1. Conaway RC, Conaway JW. The Mediator complex and transcription elongation. *Biochim. Biophys. Acta* **1829**, 69-75 (2013).
2. Hochheimer A, Tjian R. Diversified transcription initiation complexes expand promoter selectivity and tissue-specific gene expression. *Genes Dev.* **17**, 1309-1320 (2003).
3. Malik S, Roeder RG. Dynamic regulation of pol II transcription by the mammalian Mediator complex. *Trends Biochem. Sci.* **30**, 256-263 (2005).
4. Saunders A, Core LJ, Lis JT. Breaking barriers to transcription elongation. *Nat. Rev. Mol. Cell Biol.* **7**, 557-567 (2006).
5. Kwak H, Lis JT. Control of Transcriptional Elongation. *Annu. Rev. Genet.* **47**, 483-508 (2013).
6. Kong SE, Banks CA, Shilatifard A, Conaway JW, Conaway RC. ELL-associated factors 1 and 2 are positive regulators of RNA polymerase II elongation factor ELL. *Proc. Natl. Acad. Sci. USA* **102**, 10094-10098 (2005).
7. Shilatifard A, Lane WS, Jackson KW, Conaway RC, Conaway JW. An RNA polymerase II elongation factor encoded by the human ELL gene. *Science* **271**, 1873-1876 (1996).
8. Lin C*, et al.* AFF4, a component of the ELL/P-TEFb elongation complex and a shared subunit of MLL chimeras, can link transcription elongation to leukemia. *Mol. Cell* **37**, 429-437 (2010).
9. Sobhian B*, et al.* HIV-1 Tat assembles a multifunctional transcription elongation complex and stably associates with the 7SK snRNP. *Mol. Cell* **38**, 439-451 (2010).
10. He N*, et al.* HIV-1 Tat and host AFF4 recruit two transcription elongation factors into a bifunctional complex for coordinated activation of HIV-1 transcription. *Mol. Cell* **38**, 428-438 (2010).
11. Luo Z, Lin C, Shilatifard A. The super elongation complex (SEC) family in transcriptional control. *Nat. Rev. Mol. Cell Biol.* **13**, 543-547 (2012).
12. Smith ER*, et al.* The little elongation complex regulates small nuclear RNA transcription. *Mol. Cell* **44**, 954-965 (2011).
13. Hu D*, et al.* The Little Elongation Complex Functions at Initiation and Elongation Phases of snRNA Gene Transcription. *Mol. Cell* **51**, 493-505 (2013).
14. Jawdekar GW, Henry RW. Transcriptional regulation of human small nuclear RNA genes. *Biochim. Biophys. Acta* **1779**, 295-305 (2008).
15. Egloff S, O'Reilly D, Murphy S. Expression of human snRNA genes from beginning to

end. *Biochem. Soc. Trans.* **36**, 590-594 (2008).

16. Egloff S*, et al.* Serine-7 of the RNA polymerase II CTD is specifically required for snRNA gene expression. *Science* **318**, 1777-1779 (2007).
17. Baillat D, Hakimi MA, Naar AM, Shilatifard A, Cooch N, Shiekhattar R. Integrator, a multiprotein mediator of small nuclear RNA processing, associates with the C-terminal repeat of RNA polymerase II. *Cell* **123**, 265-276 (2005).
18. Medlin J, Scurry A, Taylor A, Zhang F, Peterlin BM, Murphy S. P-TEFb is not an essential elongation factor for the intronless human U2 snRNA and histone H2b genes. *EMBO J.* **24**, 4154-4165 (2005).
19. Malik S, Roeder RG. The metazoan Mediator co-activator complex as an integrative hub for transcriptional regulation. *Nat. Rev. Genet.* **11**, 761-772 (2010).
20. Takahashi H*, et al.* Human mediator subunit MED26 functions as a docking site for transcription elongation factors. *Cell* **146**, 92-104 (2011).
21. Huang Y*, et al.* Mediator complex regulates alternative mRNA processing via the MED23 subunit. *Mol. Cell* **45**, 459-469 (2012).
22. Galbraith MD*, et al.* HIF1A employs CDK8-mediator to stimulate RNAPII elongation in response to hypoxia. *Cell* **153**, 1327-1339 (2013).
23. Donner AJ, Ebmeier CC, Taatjes DJ, Espinosa JM. CDK8 is a positive regulator of transcriptional elongation within the serum response network. *Nat. Struct. Mol. Biol.* **17**, 194-201 (2010).
24. Whyte WA*, et al.* Master transcription factors and mediator establish super-enhancers at key cell identity genes. *Cell* **153**, 307-319 (2013).
25. Sato S*, et al.* A set of consensus mammalian mediator subunits identified by multidimensional protein identification technology. *Mol. Cell* **14**, 685-691 (2004).
26. Cevher MA, Shi Y, Li D, Chait BT, Malik S, Roeder RG. Reconstitution of active human core Mediator complex reveals a critical role of the MED14 subunit. *Nat. Struct. Mol. Biol.* 10.1038/nsmb.2914.
27. Tsai KL, Tomomori-Sato C, Sato S, Conaway RC, Conaway JW, Asturias FJ. Subunit architecture and functional modular rearrangements of the transcriptional mediator complex. *Cell* **157**, 1430-1444 (2014).
28. Diebold ML*, et al.* The structure of an Iws1/Spt6 complex reveals an interaction domain conserved in TFIIS, Elongin A and Med26. *EMBO J.* **29**, 3979-3991 (2010).
29. Booth V, Koth CM, Edwards AM, Arrowsmith CH. Structure of a conserved domain common to the transcription factors TFIIS, elongin A, and CRSP70. *J. Biol. Chem.* **275**, 31266-31268 (2000).
30. Devaiah BN*, et al.* Novel functions for TAF7, a regulator of TAF1-independent

transcription. *J. Biol. Chem.* **285**, 38772-38780 (2010).

31. Gegonne A*, et al.* TFIID component TAF7 functionally interacts with both TFIIH and P-TEFb. *Proc. Natl. Acad. Sci. USA* **105**, 5367-5372 (2008).
32. Kiss T. Biogenesis of small nuclear RNPs. *J. Cell Sci.* **117**, 5949-5951 (2004).
33. Marr SK, Lis JT, Treisman JE, Marr MT, 2nd. The metazoan-specific mediator subunit 26 (Med26) is essential for viability and is found at both active genes and pericentric heterochromatin in Drosophila melanogaster. *Mol. Cell. Biol.* **34**, 2710-2720 (2014).
34. Gegonne A, Weissman JD, Singer DS. TAFII55 binding to TAFII250 inhibits its acetyltransferase activity. *Proc. Natl. Acad. Sci. USA* **98**, 12432-12437 (2001).
35. Gegonne A, Weissman JD, Zhou M, Brady JN, Singer DS. TAF7: a possible transcription initiation check-point regulator. *Proc. Natl. Acad. Sci. USA* **103**, 602-607 (2006).
36. Chiang CM, Roeder RG. Cloning of an intrinsic human TFIID subunit that interacts with multiple transcriptional activators. *Science* **267**, 531-536 (1995).
37. Krebs AR, Demmers J, Karmodiya K, Chang NC, Chang AC, Tora L. ATAC and Mediator coactivators form a stable complex and regulate a set of non-coding RNA genes. *EMBO Rep.* **11**, 541-547 (2010).
38. Mourgues S*, et al.* ELL, a novel TFIIH partner, is involved in transcription restart after DNA repair. *Proc. Natl. Acad. Sci. USA* **110**, 17927-17932 (2013).
39. Kim MK, Kang YS, Lai HT, Barakat NH, Magante D, Stumph WE. Identification of SNAPc subunit domains that interact with specific nucleotide positions in the U1 and U6 gene promoters. *Mol. Cell. Biol.* **30**, 2411-2423 (2010).
40. Hutten S, Chachami G, Winter U, Melchior F, Lamond AI. A role for the CB-associated SUMO isopeptidase USPL1 in RNAPII-mediated snRNA transcription. *J. Cell Sci.* **127**, 1065-1078 (2014).
41. Kloet SL, Whiting JL, Gafken P, Ranish J, Wang EH. Phosphorylation-dependent regulation of cyclin D1 and cyclin A gene transcription by TFIID subunits TAF1 and TAF7. *Mol. Cell. Biol.* **32**, 3358-3369 (2012).
42. Marr MT, 2nd, Isogai Y, Wright KJ, Tjian R. Coactivator cross-talk specifies transcriptional output. *Genes Dev.* **20**, 1458-1469 (2006).
43. Bernues J*, et al.* Common and unique transcription factor requirements of human U1 and U6 snRNA genes. *EMBO J.* **12**, 3573-3585 (1993).
44. Zaborowska J, Taylor A, Murphy S. A novel TBP-TAF complex on RNA polymerase II-transcribed snRNA genes. *Transcription* **3**, 92-104 (2012).
45. Takahashi H, Martin-Brown S, Washburn MP, Florens L, Conaway JW, Conaway RC. Proteomics reveals a physical and functional link between hepatocyte nuclear factor

4alpha and transcription factor IID. *J. Biol. Chem.* **284**, 32405-32412 (2009).

46. Dignam JD, Martin PL, Shastry BS, Roeder RG. Eukaryotic gene transcription with purified components. *Methods Enzymol.* **101**, 582-598 (1983).

47. Morita S, Kojima T, Kitamura T. Plat-E: an efficient and stable system for transient packaging of retroviruses. *Gene Ther.* **7**, 1063-1066 (2000).

Acknowledgements

We thank Laszlo Tora (IGBMC, Strasbourg, France) for kindly providing a series of baculoviruses encoding the TBP-associated factors (TAF1-13), Michael Thirman (University of Chicago) for a generous gift of the anti-EAF1 antibody, and Yuma Nagano and Toyoyuki Ose (Hokkaido University Faculty of Pharmaceutical Sciences, Japan) and Takashi Yasukawa and Teijiro Aso (Kochi Medical School, Japan) for helpful discussion. We are grateful to Yuri Soida and Miho Uchiumi for help in preparing the manuscript. This work was supported in part by KAKENHI (24390065 to S.H.; 24689016, 24659121, 221S0002, and 25118501 to H.T.; 25280079 to I.T.) from the Ministry of Education, Culture, Sports, Science and Technology in Japan and by Takeda Science Foundation (H.T.), Osaka Cancer Research Foundation (H.T.), Mitsubishi Pharma Research Foundation (H.T.), funds from the Stowers Institute (J.W.C. and R.C.C) and grant GM41628 from NIGMS, NIH (J.W.C. and R.C.C).

Author contributions

HT planned the research, performed most of the experiments and wrote the manuscript. IT and CWS analyzed the data of ChIP-seq. WM, DA and MS performed *in vitro* binding assays. CS, SS and AR interpreted the data. TT contributed to the generation of mouse embryonic fibroblast cells. MH and YO helped with the interpretation of ChIP-seq data. MW, JWC and RCC contributed to the writing of the manuscript. SH supervised the research and contributed to the writing of the manuscript.

Competing financial interests

The authors declare that they have no conflict of interest.

Accession codes: DRA002712

Figure legends

Figure 1. Association of MED26 NTD with little elongation complex. (a) Western blotting for FLAG-immunopurified complexes from parental HeLa cells (control) and HeLa cells stably expressing FLAG-tagged MED26 wild type (WT) and N-terminal deletion mutant (CS: 421-600). (b) Western blotting for FLAG-immunopurified complexes from parental HeLa cells (control) and HeLa cells stably expressing FLAG-tagged MED26 wild type (WT) and point mutant (R61A, K62A). (c) Western blotting for FLAG-immunopurified complexes from parental 293FRT cells (control) and 293FRT cells stably expressing FLAG-tagged BTBD19 and FLAG-tagged ICE2 (NARG2).

Figure 2. Reconstitution of little elongation complex by a baculovirus expression system. (a) ICE2 (NARG2) binds to ELL in the presence of ICE1 (KIAA0947). FLAG-immunopurified complexes from baculovirus-infected Sf9 cells expressing the indicated proteins were analyzed by Western blotting. (b) ICE1 binds to EAF1 in the presence of ELL. HA-immunopurified complexes from baculovirus-infected Sf9 cells expressing the indicated proteins were analyzed by Western blotting. (c) ICE2 binds to ELL/EAF1 in the presence of ICE1. FLAG-immunopurified complexes from baculovirus-infected Sf9 cells expressing the indicated proteins were analyzed by Western blotting. (d) Proposed architecture of the components of LEC and model for MED26 NTD function as a docking site for LEC. MED26 NTD interacts with LEC through direct interaction with EAF. In turn, the MED26 C-terminal domain binds to Pol II through Mediator. The binding site for MED26 NTD on EAF is represented by black bars. (e) Silver staining of HA-ICE1-CL/FLAG-ICE2/FLAG-ELL/Myc-EAF1 complex reconstituted by the baculovirus expression system. FLAG-ELL, Myc-EAF1, FLAG-ICE2 and HA-ICE1

C-terminal fragment (CL: 1191-2266) were co-expressed in Sf9 insect cells, and the ICE1-CL/ICE2/ELL/EAF1 complex was purified by anti-HA affinity chromatography as described in the Methods section. * indicates heavy chain and light chain derived from anti-HA antibodies used in affinity purification. (f) ICE1-CL/ICE2/ELL/EAF1 complex enhances transcription elongation by Pol II. Oligo(dC)-tailed template transcription assays were performed as described in the Results and Methods sections. Arrowhead indicates the position of the nascent transcript that is synthesized in the presence of ATP, GTP and CTP and stalled at the T site.

Figure 3. MED26 is needed for the occupancy of little elongation complex at a subset of *small nuclear RNA* genes. (a, b, c and d) Depletion of MED26 decreases the occupancy of ICE1 (KIAA0947) at a subset of Pol II-transcribed *snRNA* genes. ChIP-sequence analysis was performed using triplicate ChIP samples. Genome browser track examples showing the effect of MED26 depletion on ICE1 occupancy at a subset of *snRNA* genes including *RNU4-1* and *RNU4-2* (a), *RNU5A* and *RNU5B* (b), *RNU11* (c) and *RNU12* (d) were depicted by averaging three of each sequence read from triplicate ChIPs. (e) Western blot showing Mediator, Pol II and LEC components in HEK293T cells treated with non-targeting siRNA or MED26 siRNA#1. (f) Knockdown of MED26 decreases the occupancy of ICE1, ELL, EAF2, and total and Ser7-phosphorylated Pol II at a subset of *snRNA* genes. Ct values of each ChIP were normalized to that of input. Each value is the average of three independent experiments, and error bars show standard deviation (s.d.). The *P* values for the indicated comparisons were determined by Student's *t* test (*, $P < 0.05$; **, $P < 0.01$).

Figure 4. MED26-containing Mediator is present at a subset of *snRNA* genes. (a) Diagram

of the genes and primer locations used for ChIP. (b) Occupancy of Mediator subunits MED26, MED23 and MED1 at a subset of *snRNA* genes including *RNU1*, *RNU4*, *RNU5* and *U6*, and *c-Myc* genes. Ct values of each ChIP were normalized to that of input. Data points are the average of three independent experiments, and error bars show s.d.. The *P* values for the indicated comparisons were determined by Student's *t* test (*, $P < 0.05$; **, $P < 0.01$). (c) Colocalization of MED26 (red) with coilin (green) in Cajal bodies. HeLa cells were fixed by methanol and stained with anti-MED26 and anti-Coilin antibodies. Scale bars, 2 μm.

Figure 5. MED26 is required for the expression of Pol II-transcribed *small nuclear RNA* and *small nucleolar RNA* genes. (a) MED26 depletion in cells decreases the expression of a subset of Pol II-transcribed *snRNA* and *snoRNA* genes. HEK293T cells were transfected with non-targeting siRNA as a control and each of three different siRNAs (#1, #2 and #3) targeting MED26. Total RNAs were extracted from cells and the expression of indicated genes was measured by real-time qPCR. Ct values were normalized to GAPDH. Data points are the average of three independent experiments, and error bars show s.d.. The *P* values for the indicated comparisons were determined by Student's *t* test (*, $P < 0.04$; **, $P < 0.008$). (b) MED26 wild type (wt) contributes more to the expression of a subset of *snRNA* genes than does a MED26 point mutant (mut: R61A, K62A). Total RNAs were extracted from MED26 gene-trapped MEF cells expressing HA-tagged MED26 wild type (wt) or point mutant (mut), and the expression of the indicated genes was measured by real-time qPCR. Ct values were normalized to GAPDH. Data points are the average of three independent experiments, and error bars show s.d.. The *P* values for the indicated comparisons were determined by Student's *t* test (*, $P < 0.04$; **, $P < 0.008$).

Figure 6. Similarity of EAF and TAF7 in amino acids sequence that is necessary for interaction with MED26 NTD. (a) Schematic representation of deletion mutants of human EAF1. (b) Binding ability of deletion mutants of EAF1 with MED26 NTD. The indicated recombinant proteins were expressed in Sf9 cells. Recombinant proteins of FLAG-tagged MED26-NTD derivatives were immobilized on anti-FLAG M2 agarose and were then incubated with the lysate from Sf9 cells expressing each deletion mutant of HA-tagged EAF1. After washing, bound proteins were eluted and analyzed by Western blotting. F-MED26-NTD R61A,K62A has a larger molecular weight than that of F-MED26-NTD wt since the linker between the N-terminal hexa-histidine tag and FLAG tag of MED26-NTD R61A,K62A is longer than that of MED26-NTD wt. (c) Sequence alignment of EAF and TAF7 in amino acid sequence that is required for interaction with MED26 NTD. Light green column indicates hydrophobic residues. Pink column indicates basic residues. Light blue column indicates aromatic residues. Orange column indicates neutral residues. The indicated number of amino acids is from Homo sapiens EAF1 and TAF7, respectively. (d) Schematic representation of deletion mutants of human TAF7. (e) Binding ability of deletion mutants of TAF7 with MED26 NTD. The indicated recombinant proteins were expressed in Sf9 cells. Recombinant proteins of FLAG-tagged MED26-NTD derivatives were immobilized on anti-FLAG M2 agarose and were then incubated with the lysate from Sf9 cells expressing each deletion mutant of HA-tagged TAF7. After washing, bound proteins were eluted and analyzed by Western blotting. F-MED26-NTD R61A,K62A has a larger molecular weight than that of F-MED26-NTD wt since the linker between the N-terminal hexa-histidine tag and FLAG tag of MED26-NTD R61A,K62A is longer than that of MED26-NTD wt. (f) Western blot analysis of FLAG-immunopurified complexes from parental HeLa cells (control) and HeLa cells stably expressing FLAG-tagged TAF7 full length (FL) and C-terminal deletion mutants, N243 (1-243),

N202 (1-202) and N129 (1-129).

Figure 7. Identification of TAF7 and EAF1 mutations that interfere with MED26 NTD binding. (a) Sequence alignment of EAF1, TAF7 and TAF7L in amino acid sequence that is required for interaction with MED26 NTD. Light green indicates hydrophobic residues. Pink column indicates basic residues. Light blue column indicates aromatic residues. Orange column indicates neutral residues. The residues which are substituted for alanine in order to generate mutants of EAF1 and TAF7 are surrounded by square. The indicated number of amino acids is from human EAF1 and TAF7, respectively. (b) Substitution of S262, G263, S264 and D265 to A interferes with human EAF1 interaction with MED26 NTD. Recombinant proteins of wild type (wt) or point mutant (R61A,K62A) of FLAG-tagged MED26-NTD were immobilized on anti-FLAG M2 agarose. The M2 agarose complex was incubated with recombinant proteins of HA-tagged EAF1 wild type (wt) or point mutant (mut). After washing, bound proteins were eluted and analyzed by Western blotting. (c) Substitution of S229, S230, E231 and D232 to A interferes with human TAF7 interaction with MED26 NTD. Recombinant proteins of wild type (wt) or point mutant (R61A,K62A) of FLAG-tagged MED26-NTD were immobilized on anti-FLAG M2 agarose. The M2 agarose complex was incubated with recombinant proteins of HA-tagged TAF7 wt or point mutant (mut). After washing, bound proteins were eluted and analyzed by Western blotting. (d) TAF7L does not bind to MED26 NTD. Recombinant proteins of wild type (wt) or point mutant (R61A,K62A) of FLAG-tagged MED26-NTD were immobilized on anti-FLAG M2 agarose. The M2 agarose complex was incubated with recombinant proteins of HA-tagged human TAF7 or HA-tagged mouse TAF7L. After washing, bound proteins were eluted and analyzed by Western blotting. (e) Silver staining of TFIID purified from HeLa cells stably expressing FLAG-tagged TAF7 wild type (wt) and point mutant

(mut) by anti-FLAG affinity chromatography. (f) Western blotting for FLAG-immunopurified complexes from parental HeLa cells (control) and HeLa cells stably expressing FLAG-tagged TAF7 wild type (wt) and point mutant (mut).

Figure 8. TAF7 is present at a subset of *snRNA* genes. (a) Venn diagram showing the overlap of TAF7- and ICE1 (KIAA0947)-occupied genes. (b-e) TAF7 and ICE1 are present at a subset of *snRNA* genes. Comparison of the genome browser tracks showing ICE1 and TAF7 ChIP-seq analysis. ChIP-seq tracks of ICE1 (pink) are from Fig. 3a-d. (f) Occupancy of TAF7 at a subset of *snRNA* genes. Ct values of each ChIP were normalized to that of input. Each value is the average of three independent experiments, and error bars show s.d.. The *P* values for the indicated comparisons were determined by Student's *t* test (*, $P < 0.05$; **, $P < 0.01$).

Figure 9. Depletion of TAF7 in cells increases the occupancy of LEC at Pol II-transcribed *snRNA* genes. (a) Western blot showing TAF7 and Hsp90 at 48 h after transient transfection of non-targeting (control) siRNA pool or siRNA pool targeting TAF7. (b) Effect of TAF7 depletion on transcript levels of Pol II-transcribed *snRNA* genes detected by RT-qPCR performed with total RNA from cells transfected with siRNAs. Ct values were normalized to GAPDH. Data points are the average of three independent experiments, and error bars show s.d.. The *P* values for the indicated comparisons were determined by Student's *t* test (*, $P < 0.05$; **, $P < 0.01$). (c) Schematic representation of immobilized oligo(dC)-tailed template assay. Templates immobilized on Streptavidin beads were incubated with purified recombinant protein EAF1 in the presence or absence of Mediator and/or TAF7 N243. After washing, bead-bound proteins were detected by Western blotting. (d) TAF7 interferes with EAF1 recruitment by Mediator *in vitro*. Upper panel shows immobilized oligo(dC)-tailed template assays. Assays

were performed with an oligo(dC)-tailed template, EAF1, and Mediator in the presence or absence of TAF7 N243. Lower panel shows silver staining of Mediator and HA-tagged TAF7 N243 used in the assay. Mediator (x1) and HA-TAF7 N243 (x1) contain 1 pmol of the each protein or protein complex. (e) Model of immobilized oligo(dC)-tailed template assay. TAF7 N243 inhibits EAF1 recruitment to the oligo(dC)-tailed template by MED26-containing Mediator. (f) Depletion of TAF7 increased the occupancy of ICE1 (KIAA0947), EAF2, and total Pol II at *U4-1* and *U5B* snRNA genes. Ct values of each ChIP were normalized to that of input. Data points are the average of three independent experiments; error bars show s.d.. The *P* values for the indicated comparisons were determined by Student's *t* test (*, $P < 0.05$; **, $P < 0.01$).

Figure 10. Model for MED26 and TAF7 function during *snRNA* gene transcription. In the initiation or early elongation stage, TAF7 interacts with MED26 NTD and blocks LEC recruitment by MED26. In the transition from initiation to elongation, MED26 NTD is released from TAF7 and LEC is recruited to a subset of *snRNA* genes. After LEC is recruited by MED26, MED26 hands LEC to Pol II, and thereby LEC activates productive elongation of Pol II. Binding sites for the MED26 NTD on TAF7 and EAF family members are represented by black bars. N, MED26 NTD.

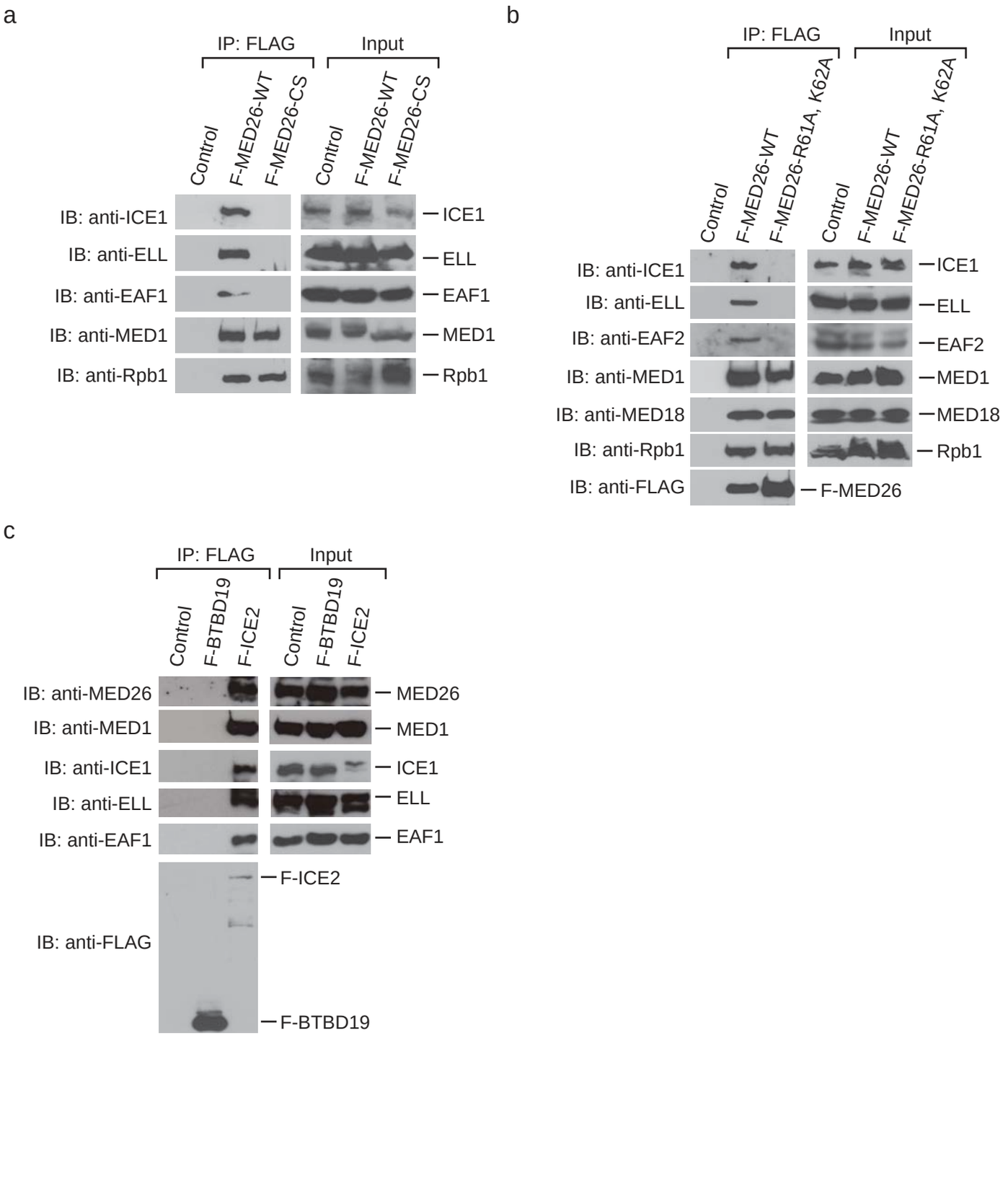
a
IP: FLAG
Input
Control
F-MED26-WT
F-MED26-CS
IB: anti-ICE1
IB: anti-ELL
IB: anti-EAF1
IB: anti-MED1
IB: anti-Rpb1
ICE1
ELL
EAF1
MED1
Rpb1
b
IP: FLAG
Input
Control
F-MED26-WT
F-MED26-R61A, K62A
IB: anti-ICE1
IB: anti-ELL
IB: anti-EAF2
IB: anti-MED1
IB: anti-MED18
IB: anti-Rpb1
IB: anti-FLAG
ICE1
ELL
EAF2
MED1
MED18
Rpb1
F-MED26
c
IP: FLAG
Input
Control
F-BTBD19
F-ICE2
IB: anti-MED26
IB: anti-MED1
IB: anti-ICE1
IB: anti-ELL
IB: anti-EAF1
IB: anti-FLAG
MED26
MED1
ICE1
ELL
EAF1
F-ICE2
F-BTBD19

Fig. 1

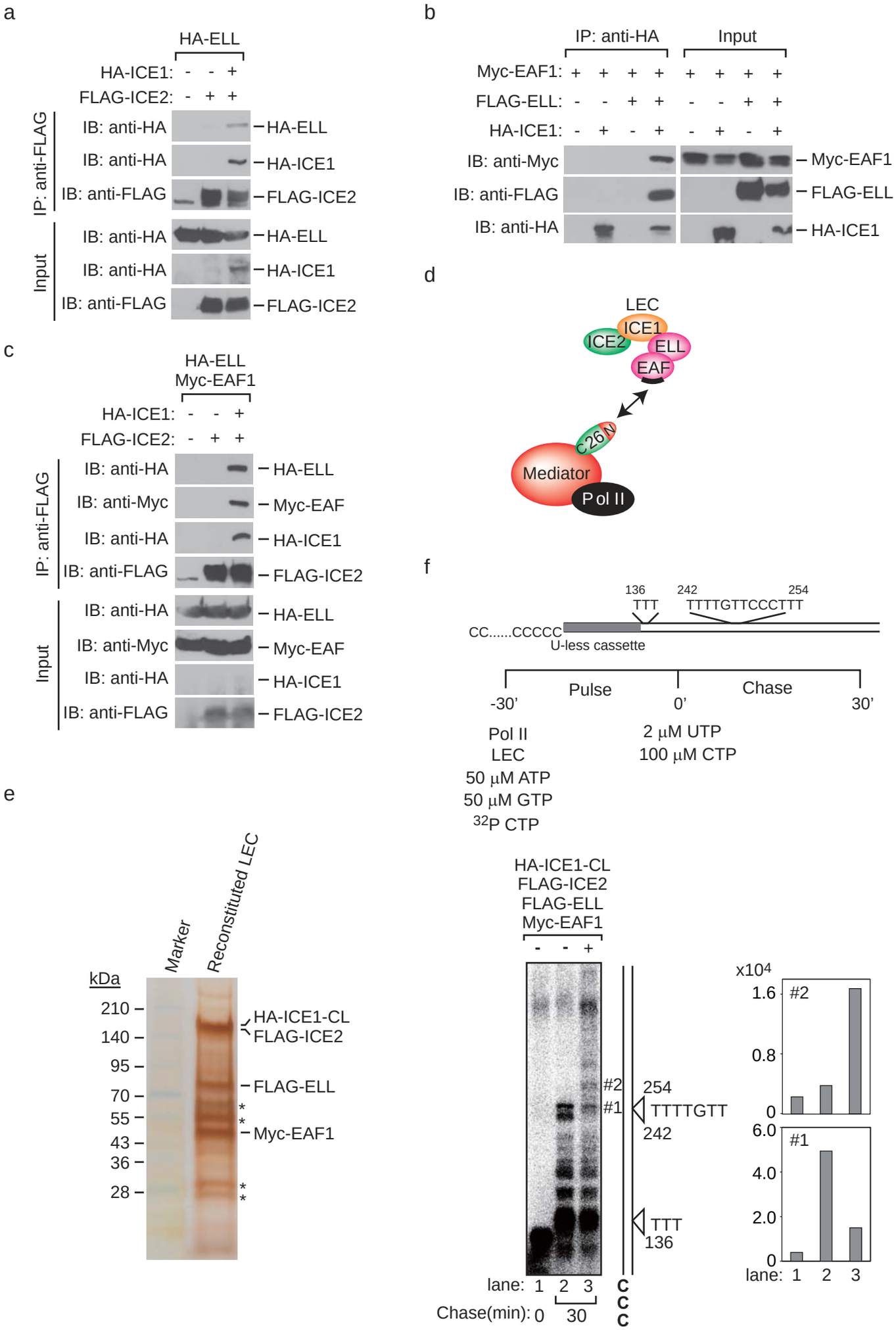
a
HA-ELL
HA-ICE1: - - +
FLAG-ICE2: - + +
IP: anti-FLAG
IB: anti-HA
HA-ELL
IB: anti-HA
HA-ICE1
IB: anti-FLAG
FLAG-ICE2
Input
IB: anti-HA
HA-ELL
IB: anti-HA
HA-ICE1
IB: anti-FLAG
FLAG-ICE2
b
IP: anti-HA
Input
Myc-EAF1: + + + + + + + +
FLAG-ELL: - - + + - - + +
HA-ICE1: - + - + - + - +
IB: anti-Myc
Myc-EAF1
IB: anti-FLAG
FLAG-ELL
IB: anti-HA
HA-ICE1
c
HA-ELL
Myc-EAF1
HA-ICE1: - - +
FLAG-ICE2: - + +
IP: anti-FLAG
IB: anti-HA
HA-ELL
IB: anti-Myc
Myc-EAF
IB: anti-HA
HA-ICE1
IB: anti-FLAG
FLAG-ICE2
Input
IB: anti-HA
HA-ELL
IB: anti-Myc
Myc-EAF
IB: anti-HA
HA-ICE1
IB: anti-FLAG
FLAG-ICE2
d
LEC
ICE1
ICE2
ELL
EAF
C26N
Mediator
Pol II
e
Marker
Reconstituted LEC
kDa
210
140
95
70
55
43
36
28
HA-ICE1-CL
FLAG-ICE2
FLAG-ELL
Myc-EAF1
f
136
242
254
TTT
TTTTGTTCCCTTT
CC.....CCCCC
U-less cassette
Pulse
Chase
-30'
0'
30'
Pol II
LEC
50 μM ATP
50 μM GTP
32P CTP
2 μM UTP
100 μM CTP
HA-ICE1-CL
FLAG-ICE2
FLAG-ELL
Myc-EAF1
- - +
#2
#1
254
TTTTGTT
242
TTT
136
lane: 1 2 3
Chase(min): 0 30
C C C
x10^4
1.6
0.8
0
#2
6.0
4.0
2.0
0
#1
lane: 1 2 3

Fig. 2

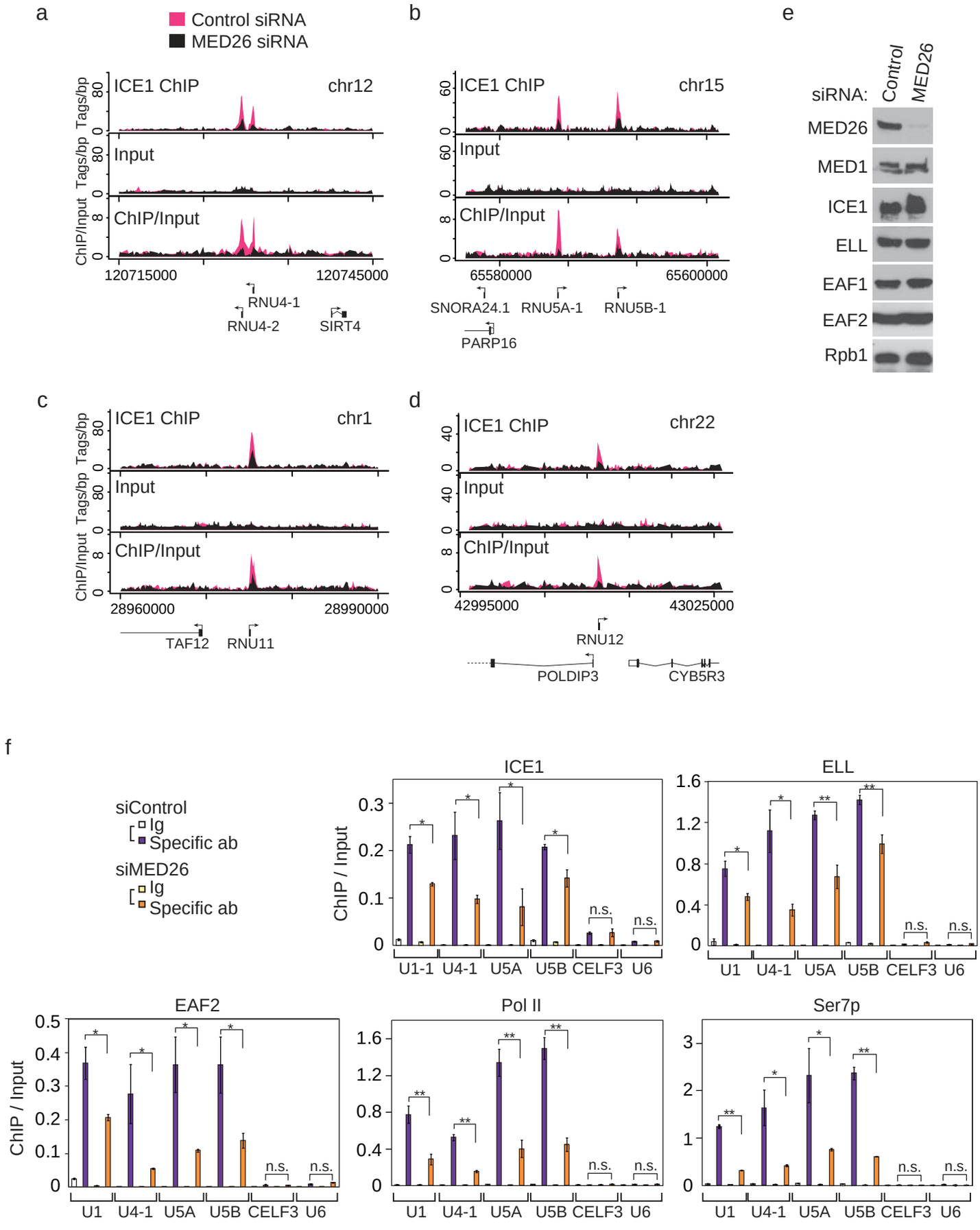
a
Control siRNA
MED26 siRNA
ICE1 ChIP
chr12
Input
ChIP/Input
Tags/bp
ChIP/Input
120715000
120745000
RNU4-1
RNU4-2
SIRT4
b
ICE1 ChIP
chr15
Input
ChIP/Input
65580000
65600000
SNORA24.1
RNU5A-1
RNU5B-1
PARP16
e
siRNA:
Control
MED26
MED26
MED1
ICE1
ELL
EAF1
EAF2
Rpb1
c
ICE1 ChIP
chr1
Input
ChIP/Input
28960000
28990000
TAF12
RNU11
d
ICE1 ChIP
chr22
Input
ChIP/Input
42995000
43025000
RNU12
POLDIP3
CYB5R3
f
siControl
Ig
Specific ab
siMED26
Ig
Specific ab
ICE1
ELL
EAF2
Pol II
Ser7p
ChIP / Input
U1-1
U1
U4-1
U5A
U5B
CELF3
U6
n.s.

Fig. 3

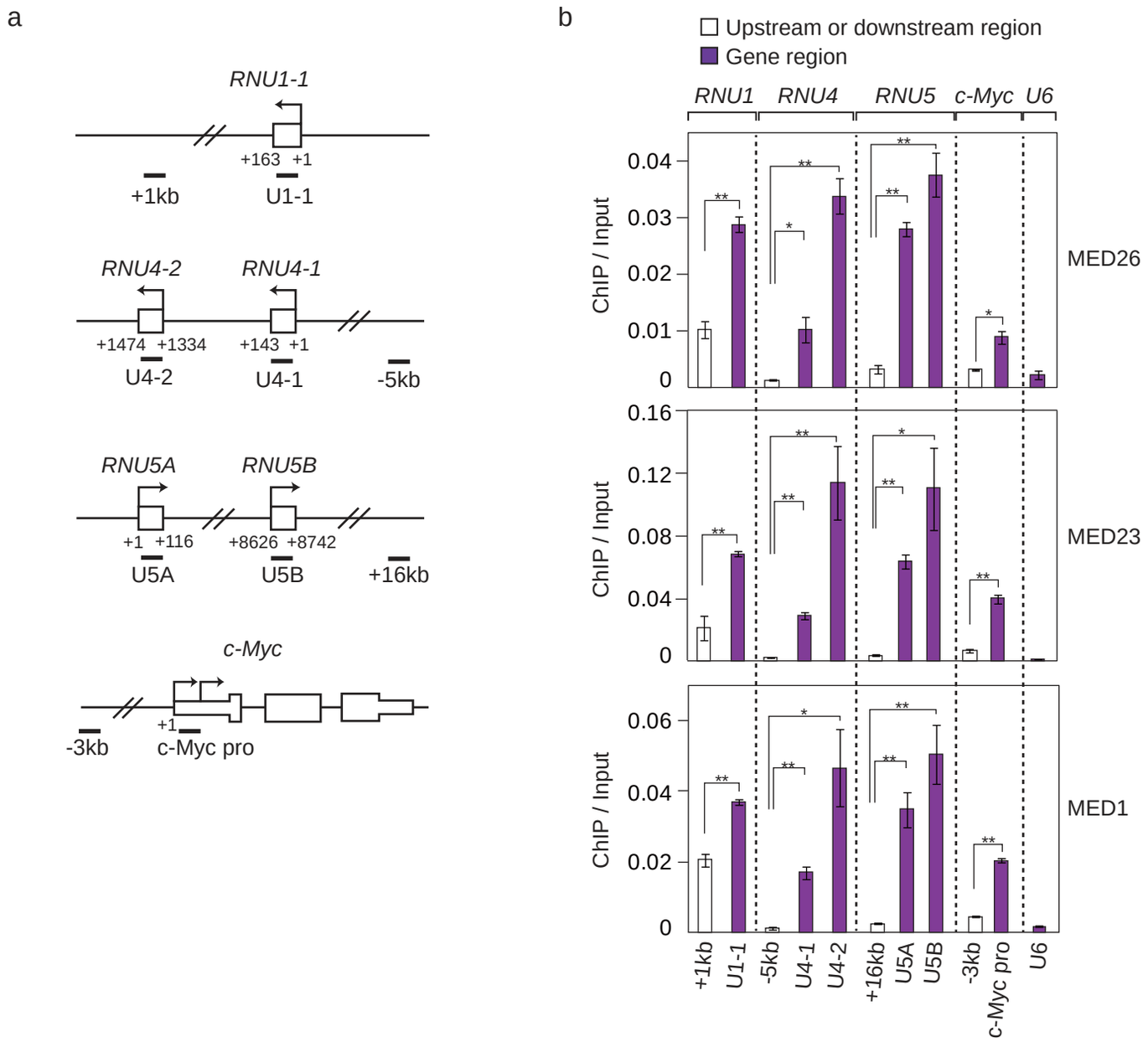
a
RNU1-1
+163 +1
+1kb
U1-1
RNU4-2
RNU4-1
+1474 +1334
+143 +1
U4-2
U4-1
-5kb
RNU5A
RNU5B
+1 +116
+8626 +8742
U5A
U5B
+16kb
c-Myc
+1
-3kb
c-Myc pro
b
Upstream or downstream region
Gene region
RNU1
RNU4
RNU5
c-Myc
U6
ChIP / Input
MED26
MED23
MED1
+1kb
U1-1
-5kb
U4-1
U4-2
+16kb
U5A
U5B
-3kb
c-Myc pro
U6
c
MED26
Coilin
DAPI
MED26 Coilin
MED26 Coilin
DAPI

Fig. 4

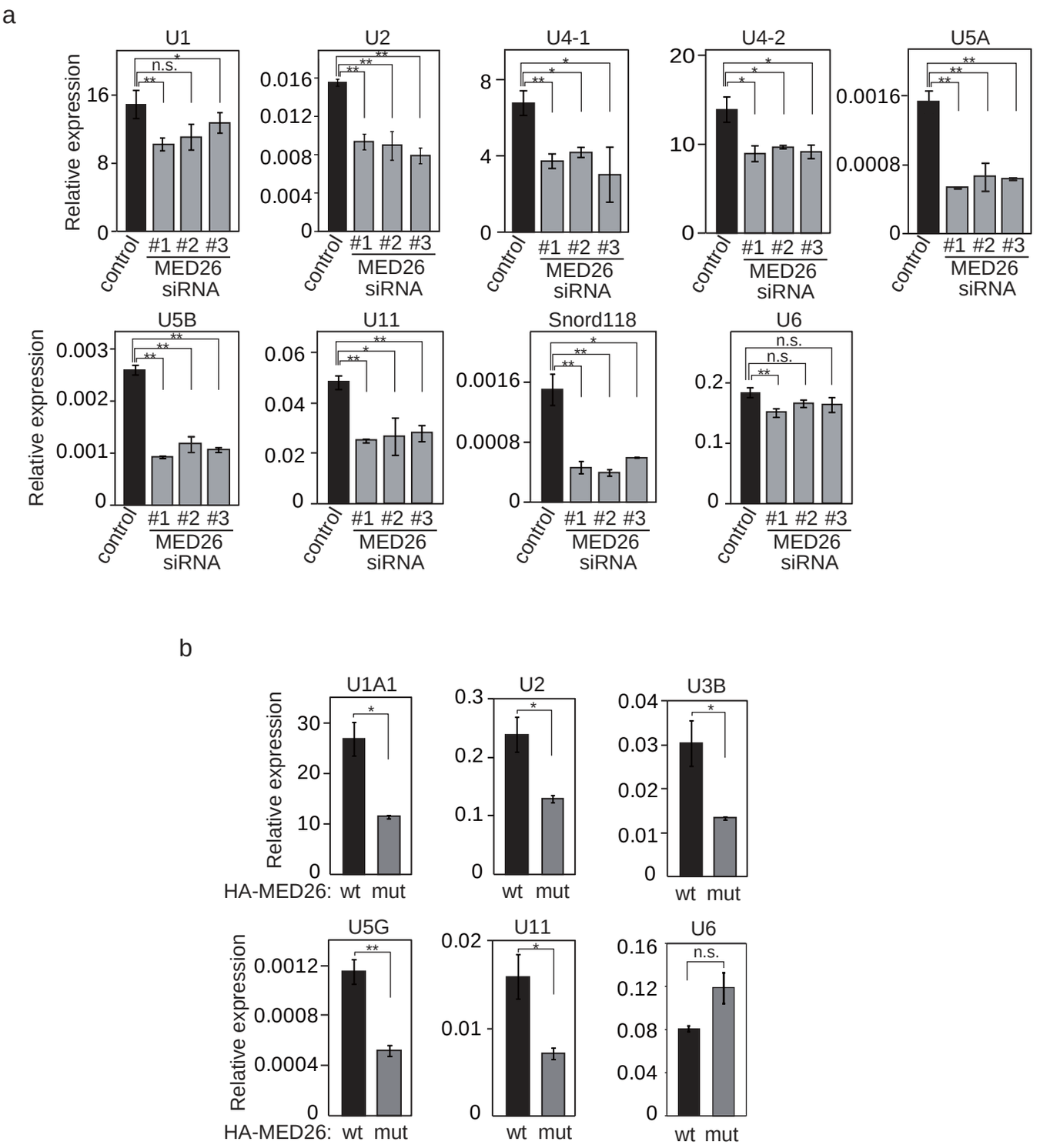
a
U1
U2
U4-1
U4-2
U5A
U5B
U11
Snord118
U6
Relative expression
n.s.
control
#1 #2 #3
MED26 siRNA
b
U1A1
U2
U3B
U5G
U11
U6
HA-MED26: wt mut
wt mut

Fig. 5

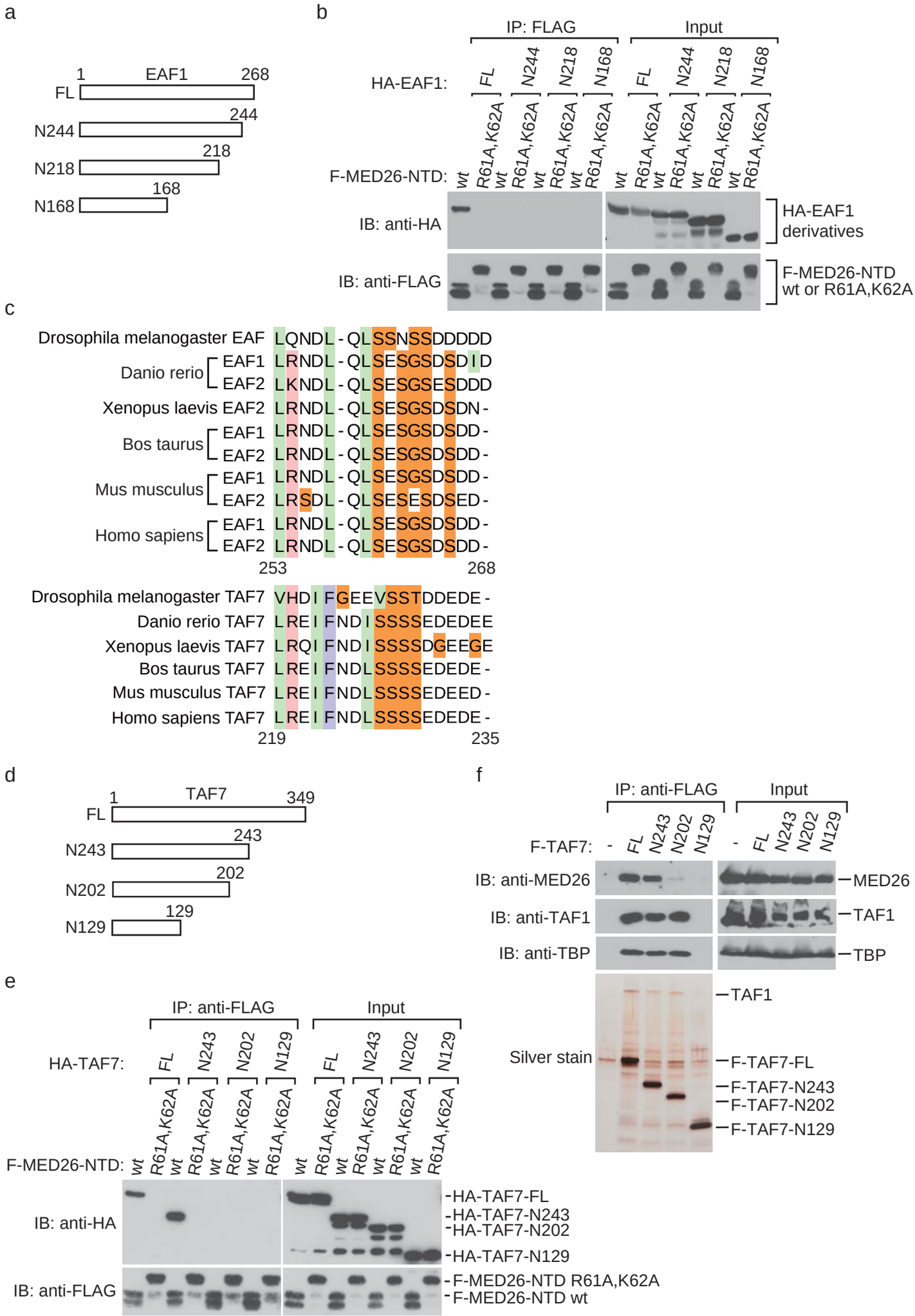
a
1
EAF1
268
FL
244
N244
218
N218
168
N168
b
IP: FLAG
Input
HA-EAF1:
FL
N244
N218
N168
R61A,K62A
F-MED26-NTD:
wt
IB: anti-HA
HA-EAF1 derivatives
IB: anti-FLAG
F-MED26-NTD wt or R61A,K62A
c
Drosophila melanogaster EAF LQNDL-QLSSNSSDDDDD
Danio rerio EAF1 LRNDL-QLSESGSDSDID
EAF2 LKNDL-QLSESGSESDDD
Xenopus laevis EAF2 LRNDL-QLSESGSDSDN-
Bos taurus EAF1 LRNDL-QLSESGSDSDD-
EAF2 LRNDL-QLSESGSDSDD-
Mus musculus EAF1 LRNDL-QLSESGSDSDD-
EAF2 LRSDL-QLSESESDSED-
Homo sapiens EAF1 LRNDL-QLSESGSDSDD-
EAF2 LRNDL-QLSESGSDSDD-
253
268
Drosophila melanogaster TAF7 VHDIFGEEVSSTDDEDE-
Danio rerio TAF7 LREIFNDISSSSEDEDEE
Xenopus laevis TAF7 LRQIFNDISSSSDGEEGE
Bos taurus TAF7 LREIFNDLSSSSEDEDE-
Mus musculus TAF7 LREIFNDLSSSSEDEED-
Homo sapiens TAF7 LREIFNDLSSSSEDEDE-
219
235
d
1
TAF7
349
FL
243
N243
202
N202
129
N129
e
IP: anti-FLAG
Input
HA-TAF7:
FL
N243
N202
N129
R61A,K62A
F-MED26-NTD:
wt
IB: anti-HA
HA-TAF7-FL
HA-TAF7-N243
HA-TAF7-N202
HA-TAF7-N129
IB: anti-FLAG
F-MED26-NTD R61A,K62A
F-MED26-NTD wt
f
IP: anti-FLAG
Input
F-TAF7:
-
FL
N243
N202
N129
IB: anti-MED26
MED26
IB: anti-TAF1
TAF1
IB: anti-TBP
TBP
Silver stain
TAF1
F-TAF7-FL
F-TAF7-N243
F-TAF7-N202
F-TAF7-N129

Fig. 6

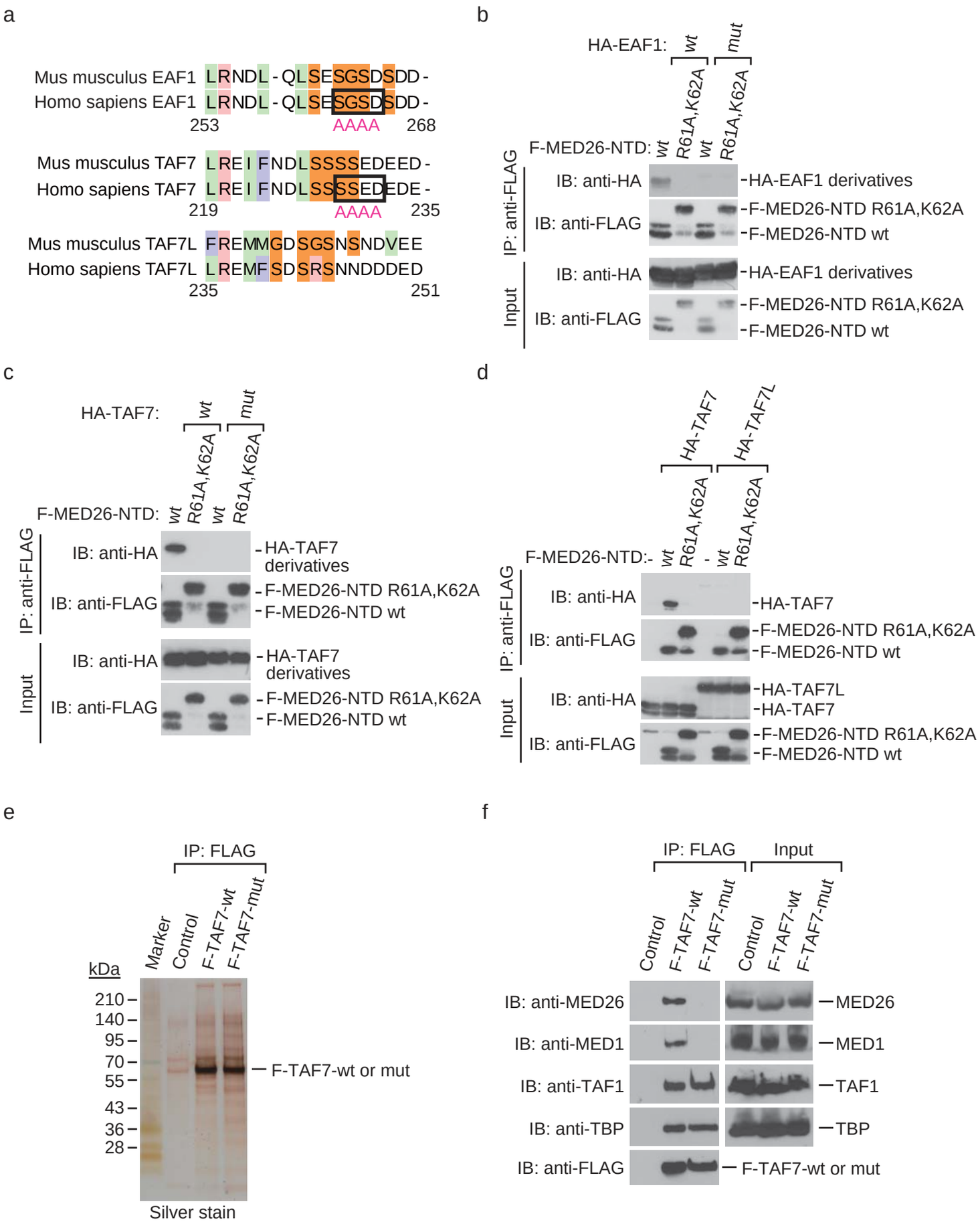
a
Mus musculus EAF1 LRNDL-QLSESGSDSDD-
Homo sapiens EAF1 LRNDL-QLSESGSDSDD-
253
AAAA
268
Mus musculus TAF7 LREIFNDLSSSSEDEED-
Homo sapiens TAF7 LREIFNDLSSSSEDEDE-
219
AAAA
235
Mus musculus TAF7L FREMMGDSGSNSNDVEE
Homo sapiens TAF7L LREMFSDSRSNNDDDED
235
251
b
HA-EAF1:
wt
mut
F-MED26-NTD:
wt
R61A,K62A
wt
R61A,K62A
IP: anti-FLAG
IB: anti-HA
HA-EAF1 derivatives
IB: anti-FLAG
F-MED26-NTD R61A,K62A
F-MED26-NTD wt
Input
IB: anti-HA
HA-EAF1 derivatives
IB: anti-FLAG
F-MED26-NTD R61A,K62A
F-MED26-NTD wt
c
HA-TAF7:
wt
mut
F-MED26-NTD:
wt
R61A,K62A
wt
R61A,K62A
IP: anti-FLAG
IB: anti-HA
HA-TAF7 derivatives
IB: anti-FLAG
F-MED26-NTD R61A,K62A
F-MED26-NTD wt
Input
IB: anti-HA
HA-TAF7 derivatives
IB: anti-FLAG
F-MED26-NTD R61A,K62A
F-MED26-NTD wt
d
HA-TAF7
HA-TAF7L
F-MED26-NTD:-
wt
R61A,K62A
-
wt
R61A,K62A
IP: anti-FLAG
IB: anti-HA
HA-TAF7
IB: anti-FLAG
F-MED26-NTD R61A,K62A
F-MED26-NTD wt
Input
IB: anti-HA
HA-TAF7L
HA-TAF7
IB: anti-FLAG
F-MED26-NTD R61A,K62A
F-MED26-NTD wt
e
IP: FLAG
Marker
Control
F-TAF7-wt
F-TAF7-mut
kDa
210
140
95
70
55
43
36
28
F-TAF7-wt or mut
Silver stain
f
IP: FLAG
Input
Control
F-TAF7-wt
F-TAF7-mut
Control
F-TAF7-wt
F-TAF7-mut
IB: anti-MED26
MED26
IB: anti-MED1
MED1
IB: anti-TAF1
TAF1
IB: anti-TBP
TBP
IB: anti-FLAG
F-TAF7-wt or mut

Fig. 7

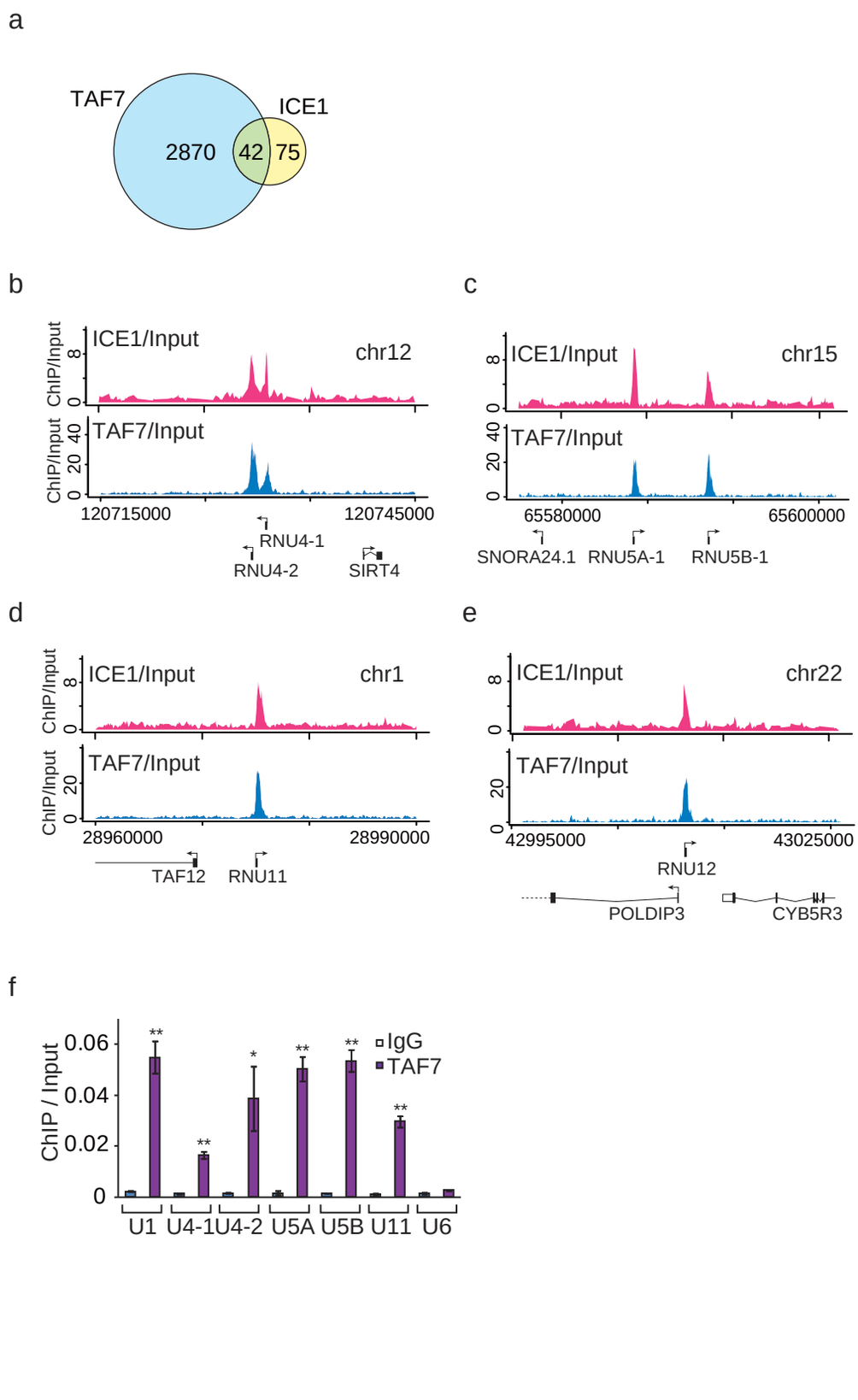
a
TAF7
ICE1
2870
42
75
b
ICE1/Input
chr12
ChIP/Input
TAF7/Input
120715000
120745000
RNU4-1
RNU4-2
SIRT4
c
ICE1/Input
chr15
TAF7/Input
65580000
65600000
SNORA24.1
RNU5A-1
RNU5B-1
d
ICE1/Input
chr1
TAF7/Input
28960000
28990000
TAF12
RNU11
e
ICE1/Input
chr22
TAF7/Input
42995000
43025000
RNU12
POLDIP3
CYB5R3
f
ChIP / Input
IgG
TAF7
U1
U4-1
U4-2
U5A
U5B
U11
U6

Fig. 8

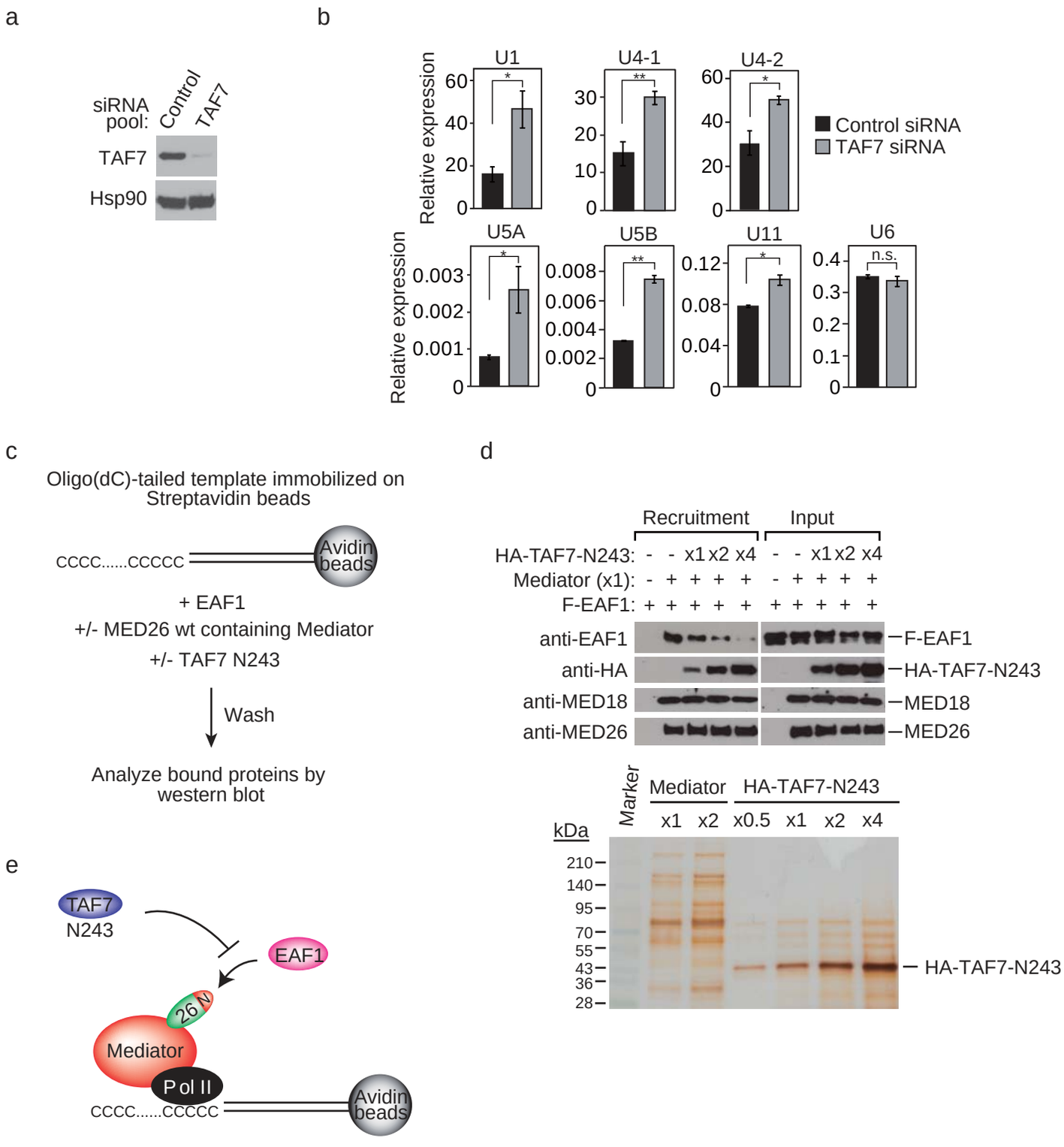
a
siRNA pool:
Control
TAF7
TAF7
Hsp90
b
Relative expression
U1
U4-1
U4-2
U5A
U5B
U11
U6
n.s.
Control siRNA
TAF7 siRNA
c
Oligo(dC)-tailed template immobilized on Streptavidin beads
CCCC.....CCCCC
Avidin beads
+ EAF1
+/- MED26 wt containing Mediator
+/- TAF7 N243
Wash
Analyze bound proteins by western blot
d
Recruitment
Input
HA-TAF7-N243: - - x1 x2 x4 - - x1 x2 x4
Mediator (x1): - + + + + - + + + +
F-EAF1: + + + + + + + + + +
anti-EAF1
anti-HA
anti-MED18
anti-MED26
F-EAF1
HA-TAF7-N243
MED18
MED26
Marker
Mediator
HA-TAF7-N243
x1 x2 x0.5 x1 x2 x4
kDa
210
140
95
70
55
43
36
28
HA-TAF7-N243
e
TAF7
N243
EAF1
26 N
Mediator
Pol II
CCCC.....CCCCC
Avidin beads
f
siControl
Ig
Specific ab
siTAF7
Ig
Specific ab
ChIP / Input
ICE1
EAF2
Pol II
n.s.
U4-1
U5B
U6

Fig. 9

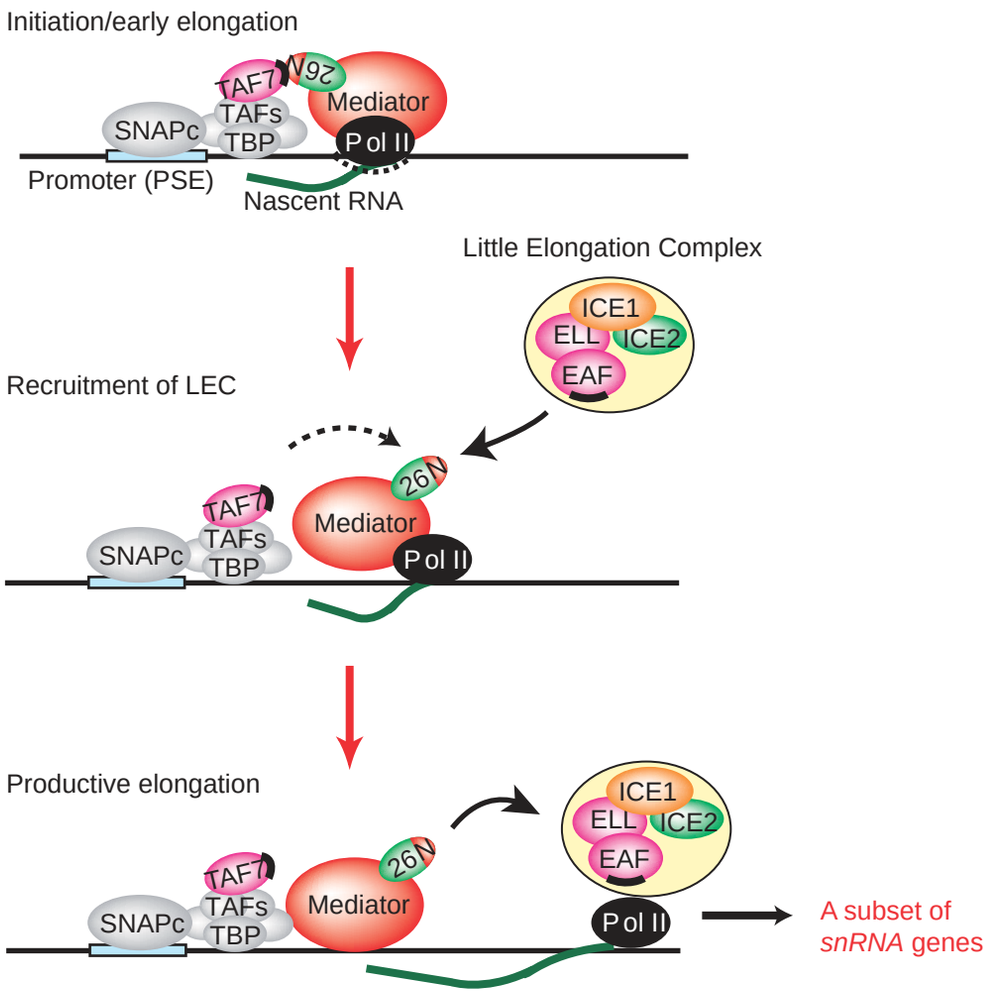
Initiation/early elongation
TAF7
26N
Mediator
TAFs
SNAPc
TBP
Pol II
Promoter (PSE)
Nascent RNA
Little Elongation Complex
ICE1
ELL
ICE2
EAF
Recruitment of LEC
Productive elongation
A subset of
snRNA genes

Fig. 10